

NUREG/CR-6077  
ORNL/TM-12416

---

---

# Data Summary Report for Fission Product Release Test VI-6

---

---

Prepared by  
M. F. Osborne, R. A. Lorenz, J. R. Travis, C. S. Webster,  
J. L. Collins

Oak Ridge National Laboratory

Prepared for  
U.S. Nuclear Regulatory Commission

9404080092 940331  
PDR NUREG  
CR-6077 R PDR



---

---

# Data Summary Report for Fission Product Release Test VI-6

---

---

Manuscript Completed: February 1994  
Date Published: March 1994

Prepared by  
M. F. Osborne, R. A. Lorenz, J. R. Travis, C. S. Webster,  
J. L. Collins

Oak Ridge National Laboratory  
Operated by Martin Marietta Energy Systems, Inc.

Oak Ridge National Laboratory  
Oak Ridge, TN 37831-6050

**Prepared for**  
**Division of Systems Research**  
**Office of Nuclear Regulatory Research**  
**U.S. Nuclear Regulatory Commission**  
**Washington, DC 20555-0001**  
**NRC FIN B0127**  
**Under Contract No. DE-AC05-84OR21400**

## Abstract

Test VI-6 was the sixth test in the VI series conducted in the vertical furnace. The fuel specimen was a 15.2-cm-long section of a fuel rod from the BR3 reactor in Belgium. The fuel had experienced a burnup of ~42 MWd/kg, with inert gas release during irradiation of ~2%. The fuel specimen was heated in an induction furnace at 2300 K for 60 min, initially in hydrogen, then in a steam atmosphere. The released fission products were collected in three sequentially operated collection trains designed to facilitate sampling and analysis.

The fission product inventories in the fuel were measured directly by gamma-ray spectrometry, where possible, and were calculated by ORIGEN2. Integral

releases were 75% for  $^{85}\text{Kr}$ , 67% for  $^{129}\text{I}$ , 64% for  $^{125}\text{Sb}$ , 80% for both  $^{134}\text{Cs}$  and  $^{137}\text{Cs}$ , 14% for  $^{154}\text{Eu}$ , 63% for Te, 32% for Ba, 13% for Mo, and 5.8% for Sr. Of the totals released from the fuel, 43% of the Cs, 32% of the Sb, and 98% of the Eu were deposited in the outlet end of the furnace. During the heatup in hydrogen, the Zircaloy cladding melted, ran down, and reacted with some of the  $\text{UO}_2$  and fission products, especially Te and Sb. The total mass released from the furnace to the collection system, including fission products, fuel, and structural materials, was 0.57 g, almost equally divided between thermal gradient tubes and filters. The release behaviors for the most volatile elements, Kr and Cs, were in good agreement with the ORNL Diffusion Model.

# Contents

Abstract .....	iii
Executive Summary .....	vii
Foreword .....	ix
1 Introduction .....	1
2 Test Description .....	3
2.1 Fuel Specimen Data .....	3
2.2 Test Conditions and Operation .....	12
2.3 Posttest Disassembly and Examination .....	18
3 Test Results .....	21
3.1 Gamma Spectrometry Data .....	21
3.2 Analysis for Iodine .....	32
3.3 Thermal Gradient Tube Deposits .....	32
3.4 Deposition of Cesium on Stainless Steel .....	35
3.5 SSMS Analyses .....	35
3.6 ICP-ES Analyses .....	39
4 Comparison of Release Data with Previous Results .....	43
5 Conclusions .....	47
6 References .....	49

## Figures

2.1 Vertical fission product release furnace, as used in test VI-6 .....	4
2.2 Vertical fission product release apparatus .....	5
2.3 Components of the fission product collection system .....	6
2.4 Details of the fuel specimen heated in test VI-6 .....	7
2.5 In-reactor release of gaseous fission products as a function of power. The gas inside rods I-830 and I-887 was measured before sectioning .....	11
2.6 Pretest gamma scan, using a 0.25-mm window, of the test VI-6 fuel specimen. Note uniform fuel burnup and radioactivity gaps between pellets .....	13
2.7 Distribution of $^{134}\text{Cs}$ , $^{137}\text{Cs}$ , and $^{154}\text{Eu}$ in the fuel and for $^{60}\text{Co}$ in the cladding of the test VI-6 fuel specimen .....	14
2.8 Temperature and collection period history for test VI-6 .....	16
2.9 Top view of open furnace after test VI-6, showing top of fuel specimen tilted to side .....	19
3.1 Distributions of fission product $^{106}\text{Ru}$ , $^{137}\text{Cs}$ , and $^{154}\text{Eu}$ in the fuel-furnace tube assembly after test VI-6 ..	22

3.2	Distribution of <sup>106</sup> Ru, <sup>125</sup> Sb, and <sup>60</sup> Co in the fuel-furnace tube assembly after test VI-6 .....	23
3.3	Release behavior of <sup>85</sup> Kr vs time and temperature in test VI-6 .....	24
3.4	Release behavior of <sup>137</sup> Cs from fuel during test VI-6, as indicated by detectors monitoring top and bottom regions of the fuel specimen .....	25
3.5	On-line distribution of released cesium forms, vapor to TGTs and aerosol to filters, compared to krypton release behavior .....	26
3.6	Distributions of <sup>137</sup> Cs along thermal gradient tubes A, B, and C in test VI-6. Note temperature profile also .....	36
3.7	Mass distribution to the collection system of material released during test VI-6 .....	38
3.8	Diffusion coefficients for <sup>85</sup> Kr, as calculated from minute-by-minute release data, in test VI-6. Note decline in diffusion coefficients with source depletion at test temperature (2310 K) .....	40
3.9	Diffusion coefficients for <sup>85</sup> Kr at constant test temperature (2310 K) in test VI-6 .....	41
4.1	Total release fractions for Kr, Cs, Ba, Te, Sb, Eu, and Mo during the three phases of test VI-6 .....	45

#### Tables

1.1	Analytical techniques used for fission product analysis .....	2
2.1	Data for fuel specimen used in test VI-6 .....	8
2.2	Fission product and actinide inventories in test VI-6: nuclides .....	9
2.3	Fission product and actinide inventories in test VI-6: elements .....	10
2.4	Operating data for test VI-6 .....	15
2.5	Chronology of test VI-6, July 11, 1991 .....	17
3.1	Summary of fission product release data for test VI-6 .....	28
3.2	Cesium release and distribution data for test VI-6 .....	29
3.3	Retention in furnace of cesium released from fuel in VI tests .....	30
3.4	Fractional release and distribution of antimony and europium in test VI-6 .....	31
3.5	Physical form of released cesium .....	32
3.6	Iodine release and distribution data for test VI-6 .....	33
3.7	Comparison of physical forms of iodine and cesium released to collection trains .....	34
3.8	Volatile iodine in test VI-6 .....	34
3.9	Vapor and aerosol deposits in test VI-6 .....	37
3.10	Test VI-6 release data for less-volatile fission products .....	39
4.1	Comparison of fission product release data for VI tests .....	44

## Executive Summary

The objective of this report is to document as completely as possible the observations and results of fission product release test VI-6 that was performed July 11, 1991. Although all analyses have not been completed and all final data have not been received, this report presents all currently available results for potential use by other reactor safety researchers. Complete interpretation and correlation of these results with related experiments and with theoretical behavior will be included in subsequent reports, which will consider the results of several tests over a range of test conditions. Similar data summary reports for previous tests in this project, as well as other reports of related project activities, are listed in the Foreword.

The fuel specimen used in this test was cut from fuel rod I-114 that had been irradiated in the BR3 reactor in Belgium from July 15, 1976, to September 26, 1980. The specimen contained 71.80 g uranium and had been irradiated to a burnup of ~42 MWd/kg uranium. The fission product inventories, as measured in the fuel and calculated by ORIGEN2, and a description of the test procedure and conditions are included in Section 3. This test was heated to the test temperature (2300 K) in a hydrogen-helium atmosphere; the Zircaloy cladding melted and ran down the vertical specimen, exposing the UO<sub>2</sub> fuel pellets. The hydrogen flow was then replaced with steam, which began to oxidize the UO<sub>2</sub>. The objective of the test was to determine the effect of steam oxidation on fission product release and transport. The test results and some preliminary interpretations are presented in Section 4, and these results are compared with data from previous tests in Section 5. The most important results are:

- (1) Posttest examination, in agreement with on-line radioactivity measurements, indicated that the Zircaloy cladding had melted during the test. The 15-cm-long fuel specimen apparently had not collapsed, however, but remained standing throughout the test.
- (2) The values for total fractional release from the fuel specimen, based on ORIGEN2 calculations and gamma-ray spectrometry measurements, were ~75% for <sup>85</sup>Kr, 64% for <sup>125</sup>Sb, 80% for both <sup>134</sup>Cs and <sup>137</sup>Cs, and 14% for <sup>154</sup>Eu. Other measurement techniques showed that 67% of the <sup>129</sup>I, 63% of the Te, 32% of the Ba, 13% of the Mo, and 5.8% of the Sr were released also. About 32% of the released <sup>125</sup>Sb, 35% of the released <sup>129</sup>I, 54% of the released Cs, and 98% of the released <sup>154</sup>Eu were deposited on the ZrO<sub>2</sub> ceramics at the outlet end of the furnace. Pretest and posttest gamma-ray spectrometry of the fuel was valuable in determining the release fractions as well as the axial distributions of the fission products within the fuel rod and the furnace.
- (3) Compared to earlier tests, both in steam (VI-1, -2, and -3) and in hydrogen (VI-4 and -5), a larger fraction of the cesium released in test VI-6 (54% vs 4 to 47%) deposited on components in the exit (top) end of the furnace. In addition, the amounts of released cesium in vapor (43 mg) and aerosol (37 mg) forms, as indicated by collection in the thermal gradient tubes (TGTs) and filters, respectively, were nearly the same in test VI-6.
- (4) The axial distributions of cesium in the test VI-6 TGTs were more uniform than in most previous tests. In TGT A (which was used during Test Phase A — the initial part of the test), a tall narrow peak indicated a high concentration of cesium at a deposition temperature of ~350°C (~625 K). No other radionuclides were detected in the TGTs except for small concentrations of <sup>125</sup>Sb and <sup>154</sup>Eu, both near the entrance of TGT C, used during Test Phase C, the final 40 min of the test.
- (5) The total mass of deposits on the TGTs and filters was determined by direct weighing to be 0.57 g; this mass was almost equally divided between the TGTs and the filters, but most of the release occurred during Test Phase C. It should be noted that the test configuration did not include reactor structural or control materials which could add significant aerosol masses during an accident.
- (6) Approximately 5.1% of the released iodine was collected in a volatile form, I<sub>2</sub>, HI, or CH<sub>3</sub>I. This relatively high fraction — in most previous tests, <0.5% of the iodine was found at this location — is believed to result from radiation decomposition of more stable forms, such as CsI.
- (7) The measured diffusion coefficients for the release of <sup>85</sup>Kr and <sup>137</sup>Cs agreed well with the ORNL Diffusion Release Model.

## Foreword

This document describes the sixth test in the VI series of fission product release tests of high-burnup, commercial LWR fuel under severe accident conditions. Similar tests at somewhat lower temperatures were conducted in the previous HI series. Other ORNL reports describing the work conducted for this project are listed below.

1. M. F. Osborne, R. A. Lorenz, J. R. Travis, and C. S. Webster, "Data Summary Report for Fission Product Release Test HI-1," NUREG/CR-2928 (ORNL/TM-8500), December 1982.
2. M. F. Osborne, R. A. Lorenz, J. R. Travis, C. S. Webster, and K. S. Norwood, "Data Summary Report for Fission Product Release Test HI-2," NUREG/CR-3171 (ORNL/TM-8667), April 1984.
3. M. F. Osborne, R. A. Lorenz, K. S. Norwood, J. R. Travis, and C. S. Webster, "Data Summary Report for Fission Product Release Test HI-3," NUREG/CR-3335 (ORNL/TM-8793), April 1984.
4. M. F. Osborne, J. L. Collins, R. A. Lorenz, K. S. Norwood, J. R. Travis, and C. S. Webster, "Data Summary Report for Fission Product Release Test HI-4," NUREG/CR-3600 (ORNL/TM-9001), June 1984.
5. M. F. Osborne, J. L. Collins, R. A. Lorenz, K. S. Norwood, J. R. Travis, and C. S. Webster, "Data Summary Report for Fission Product Release Test HI-5," NUREG/CR-4037 (ORNL/TM-9437), May 1985.
6. M. F. Osborne, J. L. Collins, R. A. Lorenz, K. S. Norwood, J. R. Travis, and C. S. Webster, "Data Summary Report for Fission Product Release Test HI-6," NUREG/CR-4043 (ORNL/TM-9943), September 1985.
7. M. F. Osborne, J. L. Collins, R. A. Lorenz, J. R. Travis, and C. S. Webster, "Design, Construction, and Testing of a 2000°C Furnace and Fission Product Collection System," NUREG/CR-3715 (ORNL/TM-9135), September 1984.
8. J. L. Collins, M. F. Osborne, R. A. Lorenz, K. S. Norwood, J. R. Travis, and C. S. Webster, "Observed Behavior of Cesium, Iodine, and Tellurium in the ORNL Fission Product Release Program," NUREG/CR-3930 (ORNL/TM-9316), February 1985.
9. K. S. Norwood, "An Assessment of Thermal Gradient Tube Results from the HI Series of Fission Product Release Tests," NUREG/CR-4105 (ORNL/TM-9506), March 1985.
10. M. F. Osborne, J. L. Collins, P. A. Haas, R. A. Lorenz, J. R. Travis, and C. S. Webster, "Design and Final Safety Analysis Report for Vertical Furnace Fission Product Release Apparatus in Hot Cell B, Building 4501," NUREG/CR-4332 (ORNL/TM-9720), March 1986.
11. M. F. Osborne, J. L. Collins, and R. A. Lorenz, "Highlights Report for Fission Product Release Tests of Simulated LWR Fuel," ORNL/NRC/LTR-85/1, February 1985.
12. Toshiyuki Yamashita, "Steam Oxidation of Zircaloy Cladding in the ORNL Fission Product Release Tests," NUREG/CR-4777 (ORNL/TM-10272), March 1988.
13. S. K. Wisbey, "Preliminary Studies of the Morphology of Thermal Gradient Tube Deposits for Fission Product Release Experiments," NUREG/CR-4778 (ORNL/TM-10273), March 1988.
14. C. S. Webster and M. F. Osborne, "The Use of Fiber Optics for Remote Temperature Measurement in Fission Product Release Tests," NUREG/CR-4721 (ORNL/TM-10366), April 1989.
15. M. F. Osborne, J. L. Collins, R. A. Lorenz, J. R. Travis, C. S. Webster, and T. Yamashita, "Data Summary Report for Fission Product Release Test VI-1," NUREG/CR-5339 (ORNL/TM-11104), June 1989.



16. M. F. Osborne, J. L. Collins, R. A. Lorenz, J. R. Travis, and C. S. Webster, "Data Summary Report for Fission Product Release Test VI-2," NUREG/CR-5340 (ORNL/TM-11105), September 1989.
17. M. F. Osborne, J. L. Collins, R. A. Lorenz, J. R. Travis, C. S. Webster, H. K. Lee, T. Nakamura, and Y.-C. Tong, "Data Summary Report for Fission Product Release Test VI-3," NUREG/CR-5480 (ORNL/TM-11399), April 1990.
18. M. F. Osborne, R. A. Lorenz, J. L. Collins, J. R. Travis, C. S. Webster, and T. Nakamura, "Data Summary Report for Fission Product Release Test VI-4," NUREG/CR-5481 (ORNL/TM-11400), October 1990.
19. M. F. Osborne, R. A. Lorenz, J. R. Travis, C. S. Webster, and J. L. Collins, "Data Summary Report for Fission Product Release Test VI-5," NUREG/CR-5666 (ORNL/TM-11743), October 1991.

## 1 Introduction

This report summarizes data from the sixth test in a vertical test apparatus. This series of tests is designed to investigate fission product release from light-water reactor (LWR) fuel in steam and/or hydrogen in the temperature range of 2000 to 2700 K. Six earlier tests, denoted HI-1 through HI-6, were conducted under similar conditions in a horizontal furnace at temperatures of 1675 to 2275 K (1400 to 2000°C). The HI series tests were analyzed and reported previously,<sup>1</sup> and comparable data summary reports are listed as items 1 through 6 in the Foreword. After revising the test apparatus to accommodate the vertical furnace, a new series of tests to higher temperatures, denoted VI-1 through VI-6, was initiated.<sup>2,6</sup> All of this work has been summarized in *Nuclear Safety*.<sup>7</sup>

The purpose of this work, which is sponsored by the U.S. Nuclear Regulatory Commission (NRC), is to obtain the experimental data needed to reliably assess the consequences of a variety of heatup accidents in LWRs.<sup>8</sup> The specific objectives of this program are:

- (1) to obtain fission product release and behavior data applicable to the analysis of reactor accidents, and
- (2) to apply these data to the development of fission product release and transport models.

Tests of high-burnup LWR fuel are emphasized in this program. The applicability of simulated fuel (unirradiated  $UO_2$  containing radioactive fission product tracers) was considered, and several simulant tests have been conducted to provide valuable data about the behavior of specific fission product species.<sup>9</sup> All tests have been conducted at atmospheric pressure in helium mixed with either steam or hydrogen in a hot cell-mounted test apparatus.

The procedures and techniques used in preparing and conducting the test, as well as in posttest examination and analysis, were very similar to those used in earlier tests. The analytical techniques employed are listed in Table 1.1. This report provides a brief description of test VI-6 and a compilation of all results obtained to date. Other analyses, in particular neutron activation for iodine, are still in process and will be reported later. Thorough data evaluation and correlation of all results from the VI test series will be included in subsequent reviews and reports covering this series of fission product release tests at temperatures up to 2700 K.

## Introduction

Table 1.1 Analytical techniques used for fission product analysis

Technique	Time	Location	Elements
Gamma spectrometry	Pretest, posttest	Fuel specimen	Long-lived, gamma-emitting fission products — Ru, Sb, Cs, Ce, Eu
	On-line	Thermal gradient tube (TGT), charcoal traps, filters	Cs, Kr
	Posttest	Furnace components, TGT, filters	Ru, Sb, Cs, Ce, Eu
Neutron activation analysis	Posttest	Charcoal; solutions from furnace, TGT, filters	I, Br
Chemical analysis	Posttest	Furnace, filters	U, Pu
Inductively coupled plasma-emission spectrometry	Posttest	Acid solutions from furnace, TGT, or filters	Many cations, especially Sr, Mo, Ru, Te, Ba, U

## 2 Test Description

The vertical test apparatus<sup>10</sup> is operated remotely and is capable of conducting tests at temperatures up to 2700 K for time periods up to 60 min in reactive atmospheres, such as steam and/or hydrogen mixed with helium. Details of the furnace are shown in Figure 2.1, and the entire test apparatus installed in the hot cell is illustrated in Figure 2.2. Both manual and automatic optical pyrometers are used for temperature measurement, supplemented by thermocouples during the low-temperature heatup phase.

The released fission products are collected in three sequentially operated, parallel collection trains. Each train is composed of (1) a 7.6-mm-ID platinum or stainless steel-lined thermal gradient tube (TGT) designed for vapor condensation; (2) a filter package containing graduated fiberglass filters for aerosol collection and heated charcoal that had been impregnated with triethylenediamine (TEDA) for iodine sorption; and (3) cold charcoal traps for rare gas collection. The on-line releases of <sup>85</sup>Kr and <sup>137</sup>Cs are monitored by detectors observing these collector components. In steam atmosphere tests, a hot CuO bed is used to oxidize the hydrogen generated by reaction of steam with the Zircaloy cladding. The collection of this water in a condenser is measured continuously by a modified conductivity meter, thereby indicating the oxidation rate of the cladding. Details of the fission product collection system are shown in Figure 2.3. Included in the test VI-6 apparatus were two radiation detectors that were collimated to monitor the radioactivity (primarily <sup>134</sup>Cs and <sup>137</sup>Cs) in the top and bottom regions of the fuel specimen. Data from these instruments should indicate any movement or collapse of the fuel during the test.

The tests planned for this vertical apparatus assumed that temperature (2000 to 2700 K) was the dominant variable. The flow rate of reactive gas (0.3 to 1.5 L/min) and time (1 to 60 min) were considered to be important but secondary variables. The objectives of this particular test were to obtain release rate data from BR3 fuel heated at 2300 K, first in hydrogen to allow cladding melting and runoff, then in steam to effect oxidation of the UO<sub>2</sub> fuel pellets, for a total time of 60 min. Test VI-2, which was heated at 2300 K in steam for 60 min, provides a basis for comparing atmospheric effects.

### 2.1 Fuel Specimen Data

The test specimen was a 15.2-cm-long section of rod I-114 from the BR3 reactor in Belgium, as shown in Figure 2.4. This fuel was irradiated from July 15, 1976, until September 26, 1980. Details of the irradiation and of the characteristics of this particular specimen were reported by Adams and Dabell<sup>7</sup> and are listed in Table 2.1. The fuel in this rod had an initial enrichment of 5.76% <sup>235</sup>U, and the VI-6 specimen had attained a burnup of ~42 MWd/kg during irradiation. Fission product inventories for the specimen were measured by direct gamma spectrometry of the fuel and were calculated with the ORIGEN2 computer program;<sup>11</sup> these data are shown in Tables 2.2 and 2.3.

As reported by Adams and Dabell, no axial scan of the gamma radioactivity along the intact fuel rod was made before the rod was sectioned. Scans of nearby rods with similar operating histories, however, indicated that rod I-114 had experienced no unusual temperature, power, or burnup histories during 1986. Reactor operating data showed that this fuel rod had operated at a maximum linear power of 222 W/cm averaged over the 1-m length, indicating that the fuel in the peak burnup region (near midlength) would have operated at a peak linear power of ~285 W/cm at that time. These data showed that the fuel had not experienced high enough operating temperatures to cause significant migration of the fission product cesium during irradiation. The data shown in Figure 2.5 were used to estimate fission gas release from the peak burnup region of a fuel rod. Using Figure 2.5 and the operating history, we estimate that ~2% of the total krypton generated in the fuel had been released during irradiation. The conversion from average gas release to release from the peak power (and peak burnup) location was made using the previously described D' (empirical) method.<sup>12</sup>

<sup>7</sup>J. P. Adams and B. R. Dabell, Idaho National Engineering Laboratory, Idaho Falls, ID 83415, "Characteristics of UO<sub>2</sub>-Zr Fuel Rods Irradiated in the BR3 Reactor," private communication, 1986.

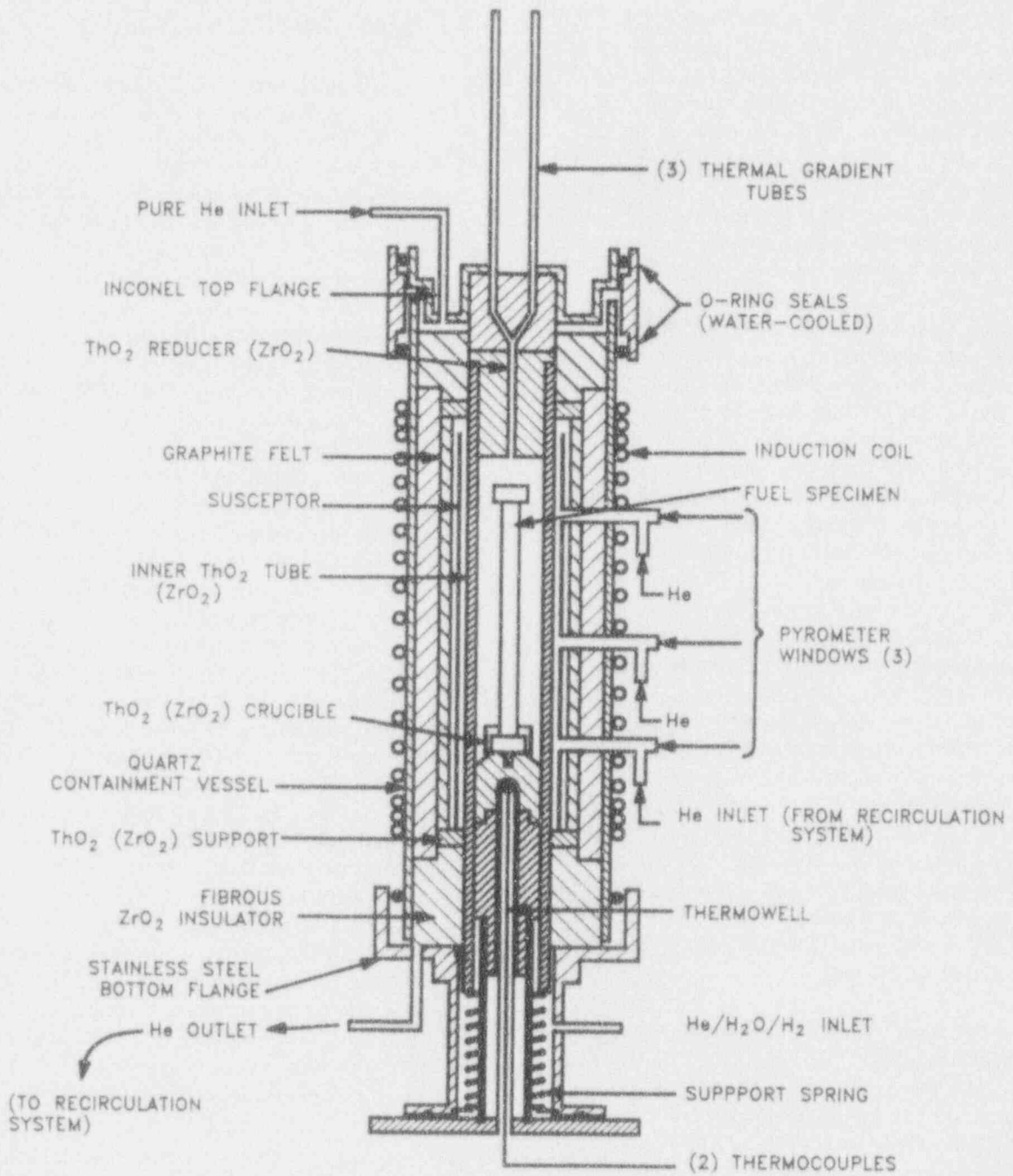


Figure 2.1 Vertical fission product release furnace, as used in test VI-6

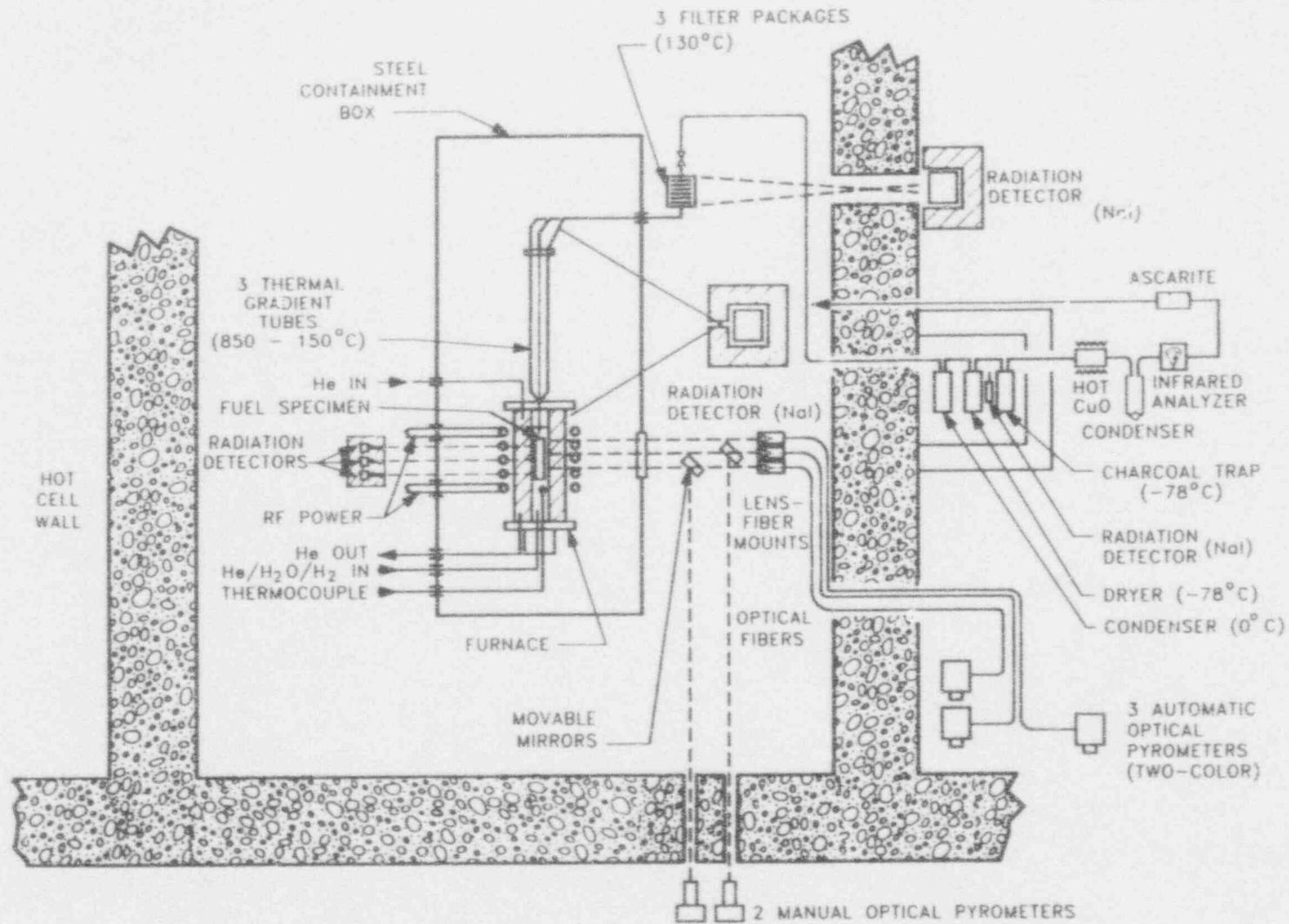


Figure 2.2 Vertical fission product release apparatus

5

NUREG/CR-6077

Description

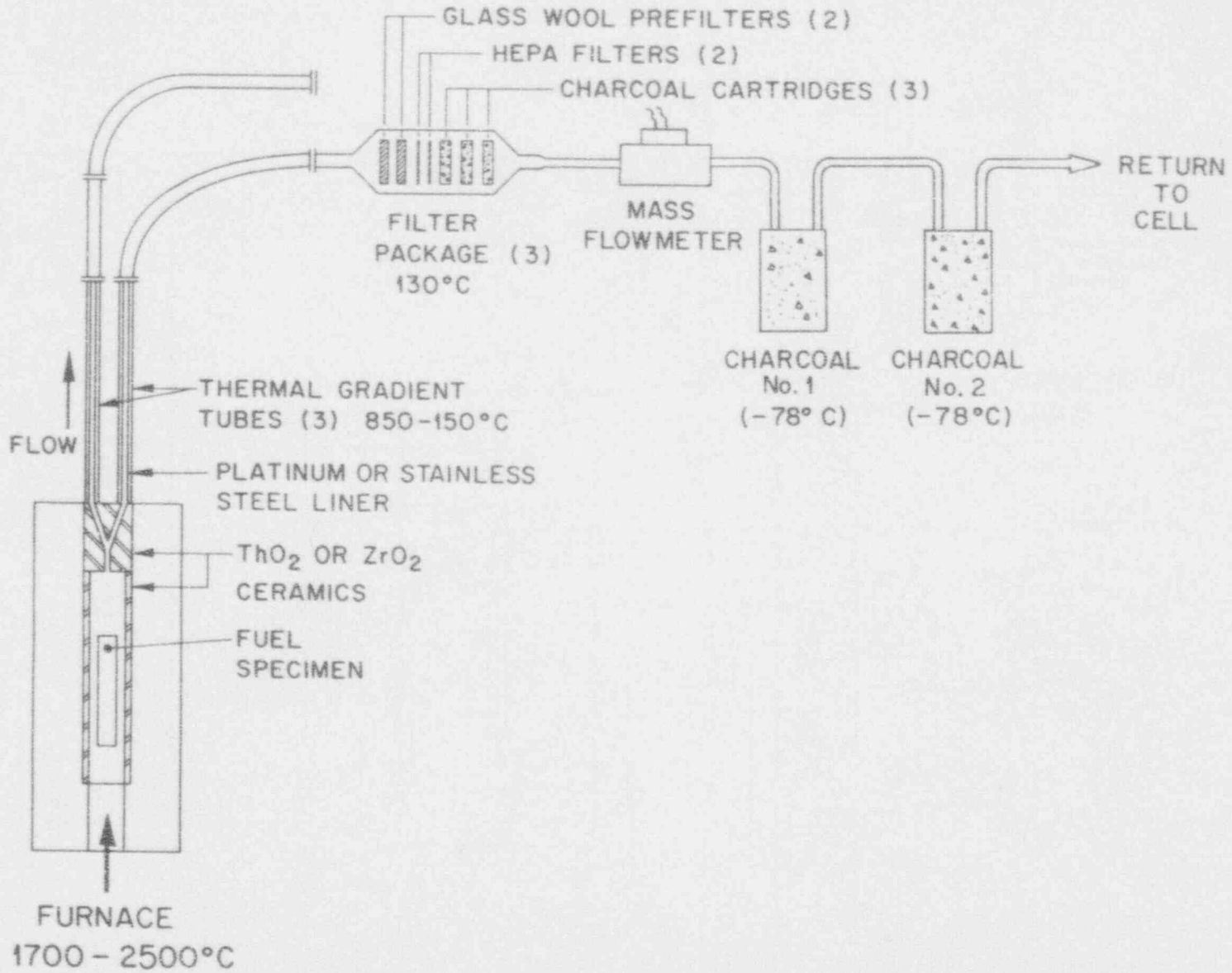


Figure 2.3 Components of the fission product collection system

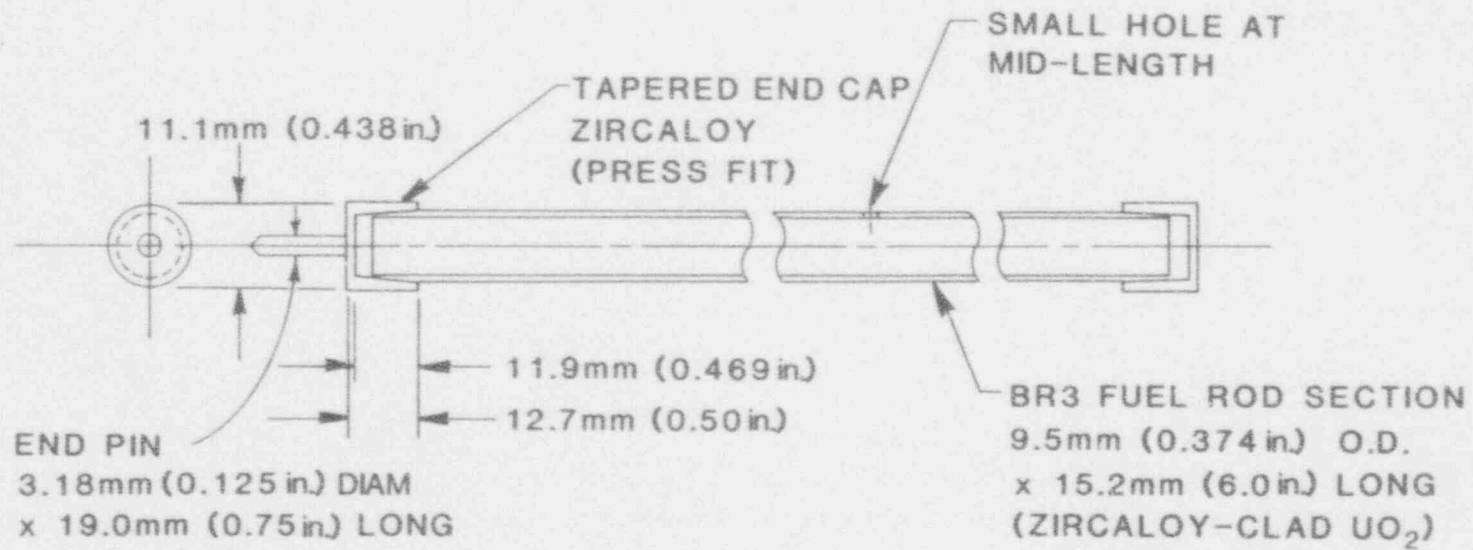


Figure 2.4 Details of the fuel specimen heated in test VI-6

7



Description

Table 2.1 Data for fuel specimen used in test VI-6

---

Fuel specimen identification	Rod I-114, section 3 BR3 Reactor (Belgium)
<b>Irradiation data</b>	
Period	July 15, 1976, to Sept. 26, 1980
Fuel specimen burnup	42 MWd/kg U
Maximum heat rating	222 W/cm
<b>Specimen data</b>	
Length	15.2 cm
Fuel loading	81.5 g UO <sub>2</sub> (71.80 g U)
Initial enrichment	5.76% <sup>235</sup> U
Total weight	103.0 g
Weight of Zircaloy	21.54 g
Gas release during irradiation	~ 2% (from specimen)

---

Table 2.2 Fission product and actinide inventories in test VI-6: nuclides

Nuclide	In VI-6 specimen*	
	(mg) At 7/1/91	(mCi) At 7/1/91
<b>Fission products</b>		
Kr-85	1.207	473.9
Sr-90	44.71	6,094
Ru-106	0.0050	16.75
Ag-110m	$7.9 \times 10^{-7}$	0.0038
Sb-125	0.0597	61.61
I-129	12.87	0.0023
Cs-134	0.259	335.5
Cs-137	88.74	7,726
Ce-144	0.0016	5.068
Eu-154	1.380	372.7
Eu-155	0.249	115.7
Total fission products	3,118	29,400
<b>Actinides</b>		
U-234	21.58	0.135
U-235	1,141	0.0025
U-236	519.6	0.034
U-238	66,090	0.0222
Total U	67,770	0.315
Pu-238	13.41	229.5
Pu-239	352.5	21.92
Pu-240	161.6	36.83
Pu-241	46.75	4,818
Pu-242	24.79	0.095
Total Pu	599.0	5,106
Total actinides	68,460	5,286

\*VI-6 specimen contained 71.80 g U = 7.180E-5 MTU before irradiation.

Table 2.3 Fission product and actinide inventories in test VI-6: elements

Element	In VI-6 specimen* (mg at 7/1/91)
Se	5.457
Br	2.097
Kr	36.87
Rb	36.30
Sr	84.08
Y	47.89
Zr	356.1
Mo	310.3
Tc	71.88
Ru	182.6
Rh	38.46
Pd	88.32
Ag	4.425
Cd	6.266
In	0.184
Sn	6.381
Sb	1.495
Te	40.03
I	15.92
Xe	474.7
Cs	232.6
Ba	152.7
La	114.1
Ce	223.4
Eu	10.91
Total fission products	3,118
U	67,770
Pu	599
Total actinides	68,460

\*VI-6 specimen contained 71.80 g U = 7.180E-5 MTU before irradiation.

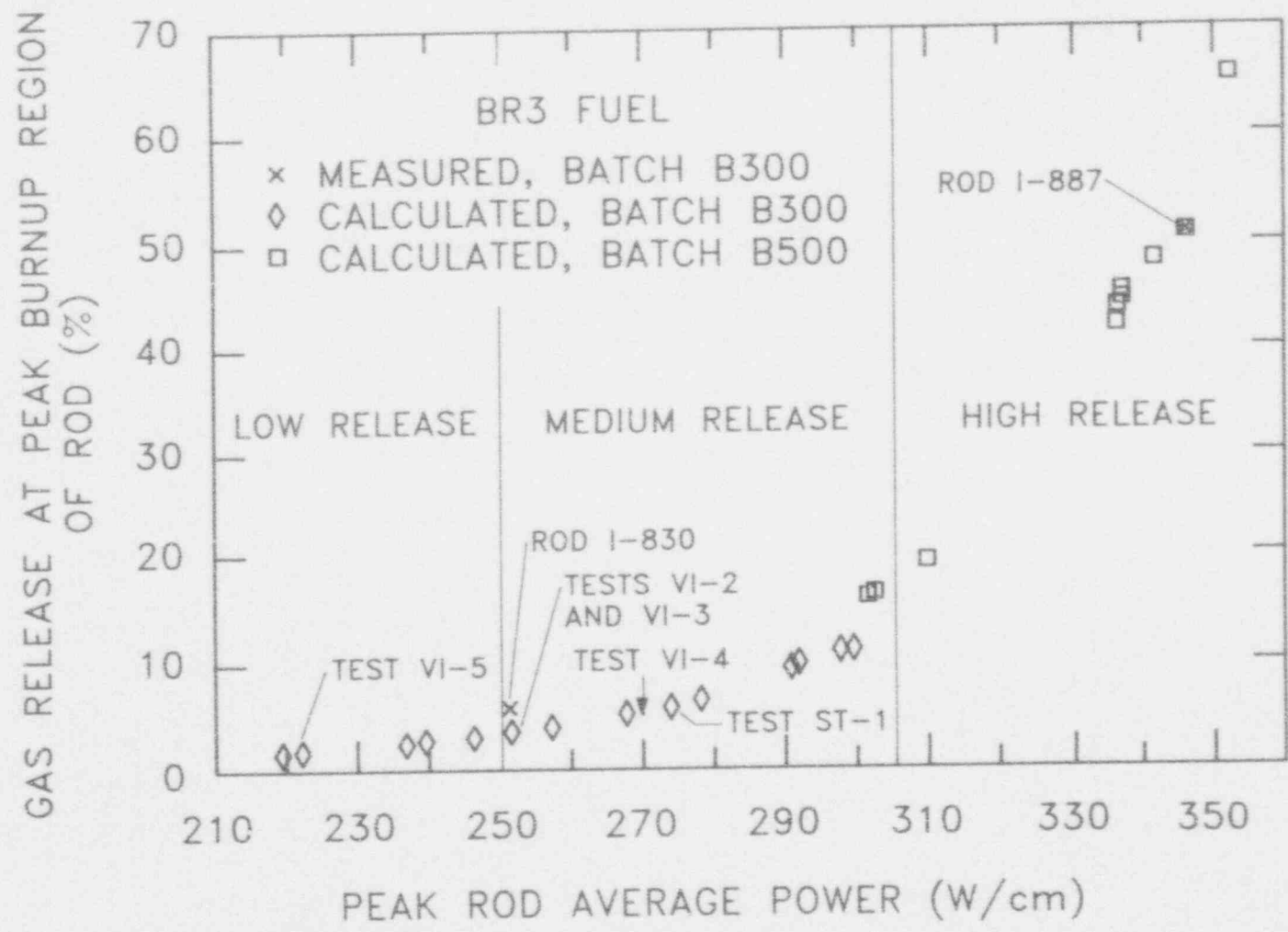


Figure 2.5 In-reactor release of gaseous fission products as a function of power. The gas inside rods I-830 and I-887 was measured before sectioning

## Description

In addition to the test VI-6 fuel specimen, three other 15.2-cm-long specimens were cut from rod I-114 and prepared for future testing. One of these specimens was heated in test VI-5.<sup>6</sup> Three short samples (1 to 2 cm long) were cut for metallographic examination, for dissolution and chemical analysis, and as an archive sample for possible future use.

Tapered end caps of Zircaloy-2 were pressed onto the ends of the test specimen, not as gas seals, but to prevent loss of the fractured  $\text{UO}_2$  fuel during subsequent handling. The bottom end cap included a pin to facilitate vertical mounting. A small hole, 1.6 mm in diameter, was drilled through the cladding at mid-length to serve as a standard leak for gas release during the heatup phase of the test. These details are shown in Figure 2.4.

The gamma-ray profile of the test VI-6 fuel specimen, as observed through a 0.25-mm (0.010-in.) window, is shown in Figure 2.6. This profile, which is dominated by  $^{134}\text{Cs}$  and  $^{137}\text{Cs}$ , indicates very uniform burnup of the fuel and fission product content along the specimen, as well as the location of individual fuel pellets. The axial distributions of  $^{134}\text{Cs}$ ,  $^{137}\text{Cs}$ ,  $^{154}\text{Eu}$ , and  $^{60}\text{Co}$ , as measured through a 1-cm window at 1-cm intervals, are shown in Figure 2.7. These data show that no significant migration of the volatile cesium occurred during irradiation.

## 2.2 Test Conditions and Operation

As in each of the previous experiments, the test apparatus was assembled by direct handling, which is possible because the hot cell and test apparatus are decontaminated after each test. Also, new  $\text{ZrO}_2$  furnace components, new TGT liners of 0.002-in. (0.051-mm)-thick stainless steel, and new filter package components were prepared and installed. In most previous tests, platinum liners were used to provide a relatively unreactive surface for the deposition of fission products, so that effects on the chemical forms of the deposits would be minimized. In an effort to investigate the effects of a realistic reactor material on the forms of the deposits, stainless steel liners were used in test VI-6 and in some earlier tests. Only the transfer and loading of the highly radioactive fuel

specimen and the final closure of the furnace and containment box were done remotely. No in-cell operations were required during the test. Before heating was begun, the test apparatus was evacuated and purged with helium.

This test was intended to study the effect of steam oxidation of the  $\text{UO}_2$  on fission product release at 2300 K. In earlier tests in steam, VI-1, VI-2, and VI-3, the oxidized cladding had remained largely intact, serving as a barrier to effective  $\text{UO}_2$ -steam contact. The operating conditions are summarized in Table 2.4, and the temperature history similar to that in test VI-2 is shown in Figure 2.8. The heatup rate in test VI-6 was  $\sim 0.8$  K/s, which is similar to those in tests VI-1 and VI-2. Tests using  $\text{ThO}_2$  ceramic furnace tubes (VI-3 and VI-5) required slower heatup rates to avoid fracturing by thermal shock.

The more important events during the test are listed in the test chronology, Table 2.5. The time periods for operation of the three collection trains (see Figure 2.8) were for Train A, 0 to 55 min; for Train B, 55 to 73 min; and for Train C, 73 min to the end of the test,  $\sim 200$  min, including cooldown. A preheat period was included to slowly heat the specimen to  $\sim 550$  K in helium prior to beginning hydrogen flow to the furnace. Time zero was defined as that time when the controlled heating ramp was begun, with stable gas (hydrogen + helium) flow through the warm furnace established. Temperature measurement and control were generally good. The 12-min period at  $\sim 1400$  K was included to ensure heatup of ceramics in the outlet end of the furnace and to compare the data from the optical pyrometers before any significant release of fission products had occurred.

With one exception, operation of test VI-6 was conducted as planned. At the transition from Test Phase A (hydrogen + helium atmosphere) to Test Phase B (steam + helium atmosphere), the valves for switching the flows of reactive gases were operated correctly, but a partially open bypass valve allowed most of the steam to escape from the system, rather than to flow through the furnace as planned. This loss of steam was detected and corrected at a test time of 93 min, 20 min into Test Phase C.

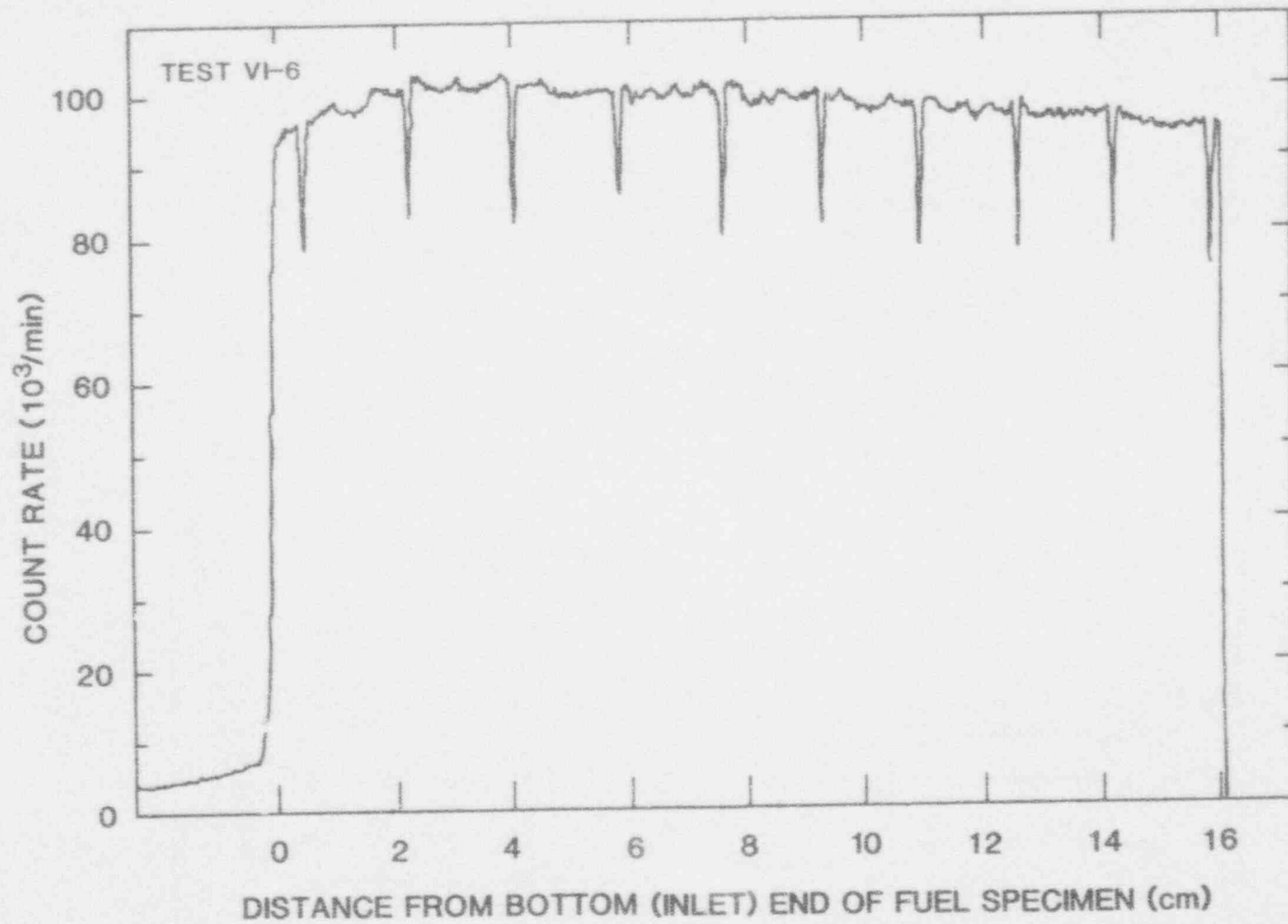


Figure 2.6 Pretest gamma scan, using a 0.25-mm window, of the test VI-6 fuel specimen. Note uniform fuel burnup and radioactivity gaps between pellets

FISSION PRODUCT CONCENTRATION IN FUEL  
(arbitrary units)

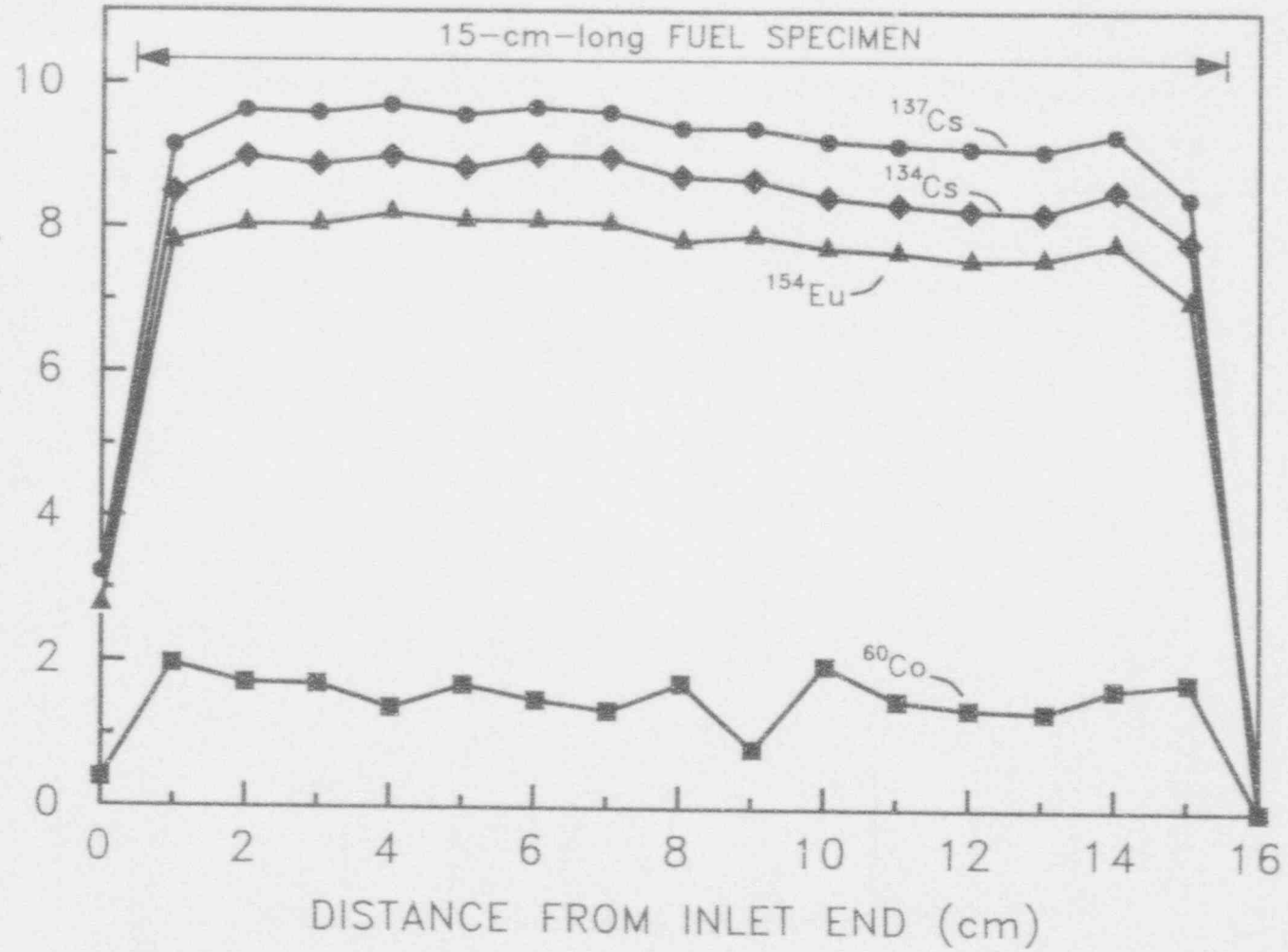


Figure 2.7 Distribution of <sup>134</sup>Cs, <sup>137</sup>Cs, and <sup>154</sup>Eu in the fuel and for <sup>60</sup>Co in the cladding of the test VI-6 fuel specimen

Table 2.4 Operating data for test VI-6

<b>Specimen temperature (K)</b>	
At start of heatup ramp	~ 570
During 10-min period to check pyrometers	1415
During 60-min period (Phases A, B, and C)	2310
Heatup rate of Phase A	0.83 K/s
Cooldown rate	0.60 K/s
Time above 2000 K	72 min
<b>Nominal gas flow rate data (L/min at 20°C, 1 bar)<sup>*,**</sup></b>	
<u>During Phase A</u>	
50% H <sub>2</sub> + He recirculation system	0.20
50% H <sub>2</sub> + He to fuel specimen	0.80
<u>During Phases B and C</u>	
He to recirculation system	0.20
He to fuel specimen	0.30
Steam to fuel specimen	1.0 <sup>+</sup>
Recirculation/purification system	1.5

\*Measured by mass flowmeters.

\*\*Absolute pressure in furnace during test was 0.09906 MPa (742 mm Hg).

+During Phase B and first 17 min of Phase C, steam flow across fuel specimen was reduced by an unknown amount because of leakage.



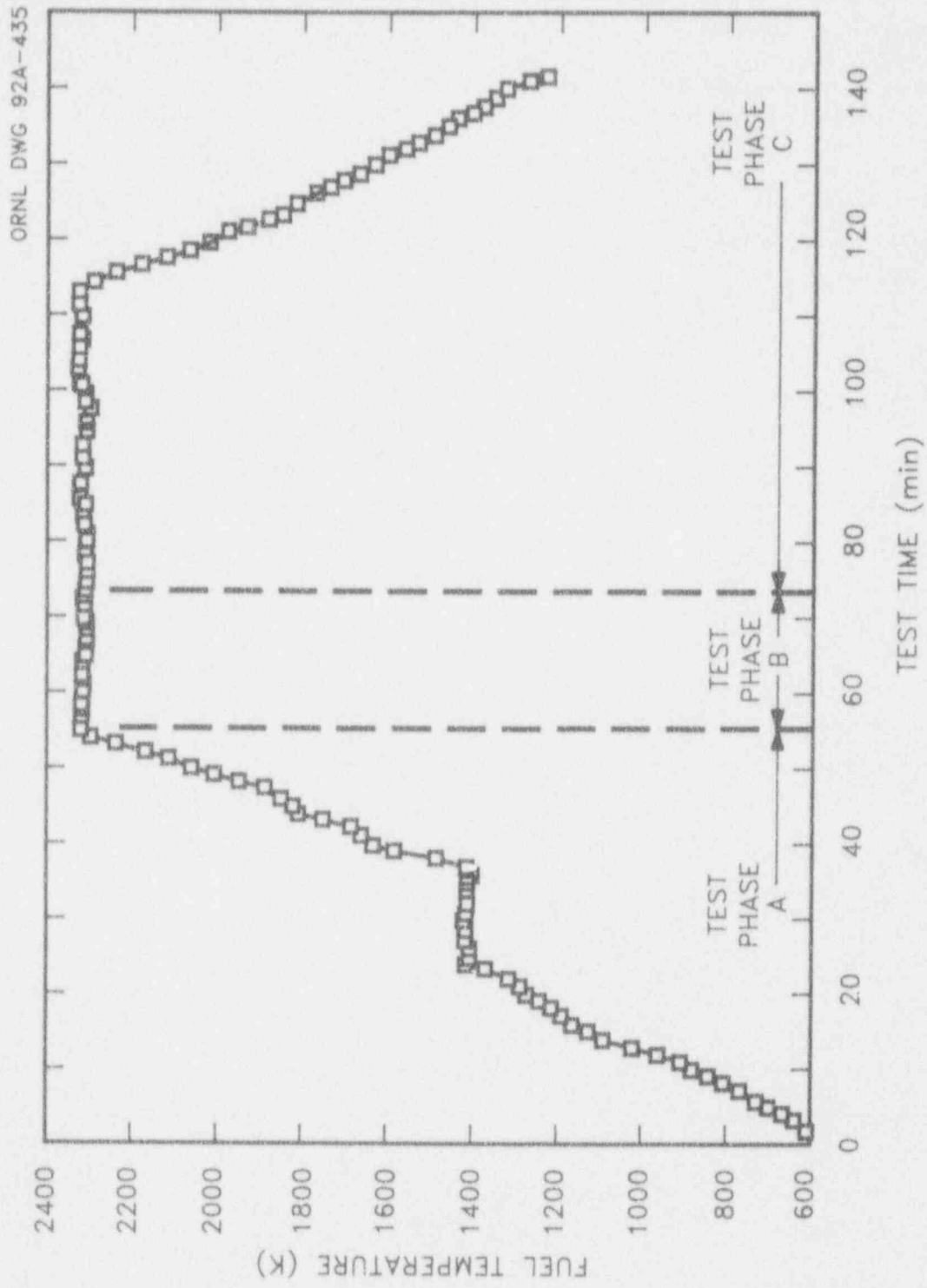


Figure 2.8 Temperature and collection period history for test VI-6

Table 2.5 Chronology of test VI-6, July 11, 1991

Event/observation	Time		Furnace temperature corrected (K)
	Clock (h)	Test (min)	Center
Load fuel into furnace	2015*		RT**
Complete leak checks	2100*		RT
Begin system preheat, TGTs and filters	1000		RT
Begin furnace preheat with gas flow to furnace	1155		RT
Stable flow and temperature	1330		620*
<b>Test Phase A</b>			
Start ramp to ~1400 K	1445	0	606*
First Micro No. 1 T measurement	1458	13	1088
Reached ~1400 K plateau	1508	23	1420
Resume ramp to 2300 K, observed Kr release	1520	35	1406
First Cs detected, on TGT	1525	40	1668
Rapid Kr release, Cs on filter	1527	42	1750
Reached 2300 K plateau, hold 2 min	1538	53	2294
End Phase A, stop H <sub>2</sub> flow, begin steam flow	1540	55	2318
<b>Test Phase B</b>			
Begin Phase B, hold 18 min	1540	55	2318
End Phase B	1558	73	2306
<b>Test Phase C</b>			
Begin Phase C, hold 40 min	1558	73	2306
Closed steam leak	1616	91	2314
End 2300 K plateau, reduce power to cool	1638	113	2323
Cooling rate ~50/min	1644	119	2023
Turn power off	1646	121	1933
Cooling rate ~35/min	1650	125	1766
Cooling rate ~30/min	1700	135	1437
Last pyrometer measurements	1708	143	1226
Test essentially complete	1718	153	~1000*
End Phase C, stopped gas flow	1807	202	~450*

\*July 10, 1991.

\*\*RT = room temperature.

+Based on thermocouple measurement.

## Description

### 2.3 Posttest Disassembly and Examination

After the test was completed, the apparatus was monitored for the distribution of radioactivity before disassembly was begun. The highest concentrations of radioactivity were found at the furnace exit and in the first (lower) half of the TGTs. Initially, the filter assemblies and the top furnace flange-TGT assembly, containing the TGT liners, were removed, sealed, and transferred to another hot cell to avoid potential

contamination from fuel handling. The  $ZrO_2$  top end plug was removed from the furnace tube to allow observation of the interior. The photo in Figure 2.9 shows a top view of the open furnace with the  $UO_2$  fuel column tilted to one side but still standing. After photography, the furnace cavity was filled with epoxy resin to preserve the geometry of the degraded fuel specimen during handling and any sectioning and microstructural examination. After removal of the fuel-furnace tube assembly from the furnace, it was analyzed in detail by gamma spectrometry.

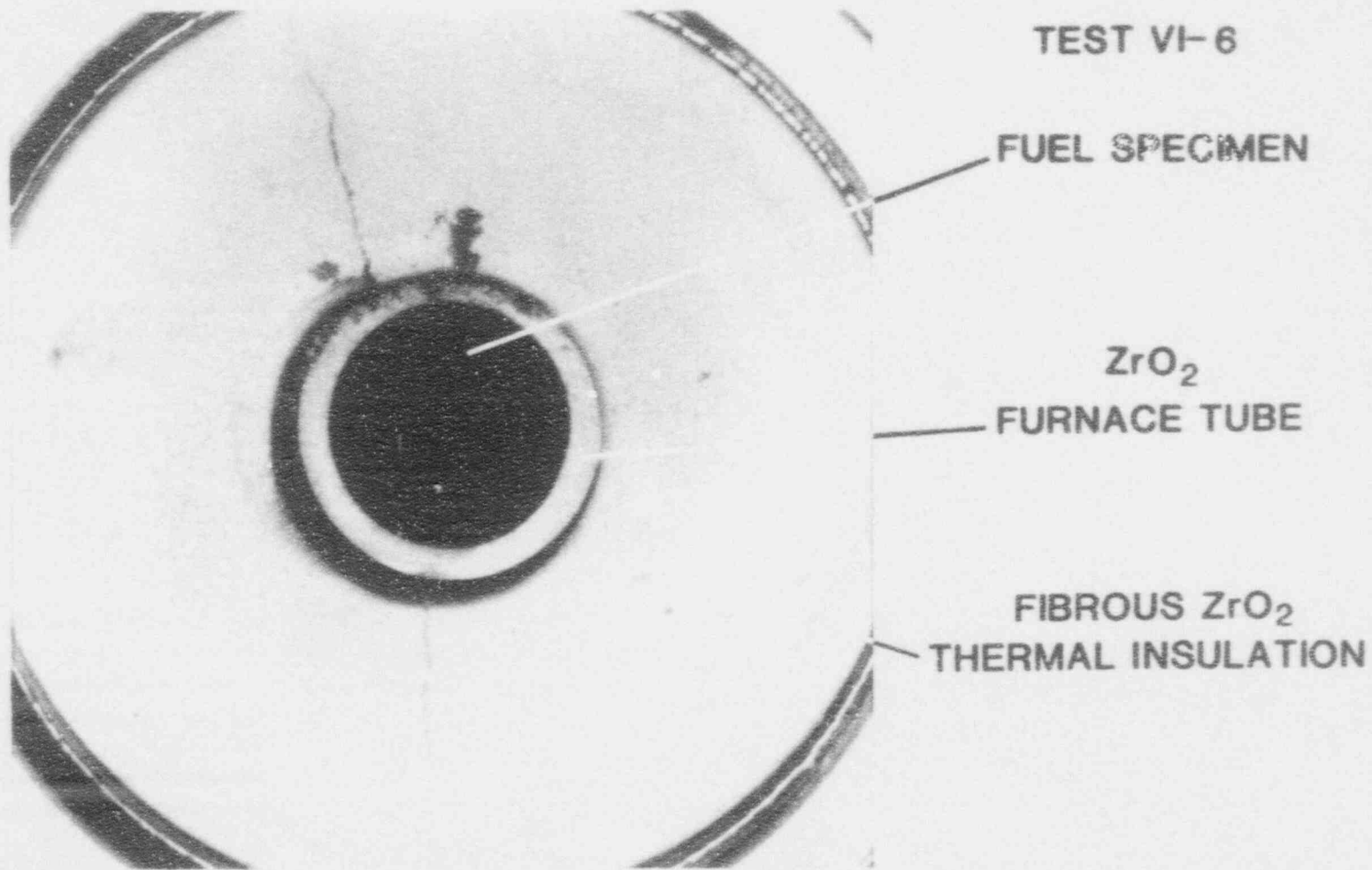


Figure 2.9 Top view of open furnace after test VI-6, showing top of fuel specimen tilted to side

01010

### 3 Test Results

#### 3.1 Gamma Spectrometry Data

After the test, all experimental components and collectors were analyzed under well-defined geometry to determine the concentration of the gamma-emitting fission products. The previously proven empirical method of determining the effective shielding to obtain a mass balance for cesium among several of the  $^{134}\text{Cs}$  gamma-ray energies was used.<sup>2</sup>

Pretest gamma spectrometric analysis of the 15.2-cm-long fuel specimen was used to determine the fission product inventories in the fuel. Long-lived gamma emitters —  $^{106}\text{Ru}$ ,  $^{125}\text{Sb}$ ,  $^{134}\text{Cs}$ ,  $^{137}\text{Cs}$ ,  $^{154}\text{Eu}$ , and  $^{60}\text{Co}$  — were determined directly. A calculation by the computer program ORIGEN2 supplied the inventory values for other fission products, activation products, and fuel nuclides, as shown in Tables 2.2 and 2.3. Based on measurements at 1-cm intervals of the  $^{134}\text{Cs}$ ,  $^{137}\text{Cs}$ , and  $^{154}\text{Eu}$ , as shown in Figure 2.7, the axial distributions of the major fission products were relatively uniform along the rod. The uniform axial distribution of the  $^{60}\text{Co}$  in the Zircaloy cladding, also shown in Figure 2.7, is further verification of a uniform neutron dose (which indicates a similar burnup distribution) during irradiation.

The posttest distributions of  $^{106}\text{Ru}$ ,  $^{137}\text{Cs}$ , and  $^{154}\text{Eu}$ , as determined by gamma analysis of 1-cm-long sections of the fuel-furnace tube assembly, are shown in Figure 3.1, and the corresponding data for  $^{106}\text{Ru}$ ,  $^{125}\text{Sb}$ , and  $^{60}\text{Co}$  are shown in Figure 3.2. In the region where the fuel was originally located (0 to 15.2 cm in both figures), the dominant species were  $^{106}\text{Ru}$  and  $^{154}\text{Eu}$ . However, relocation of all gamma emitters is apparent. Firstly, most of the  $^{137}\text{Cs}$  had been released from the hot zone of the furnace, with the remainder distributed over the original fuel zone (presumably in the  $\text{UO}_2$  fuel) at ~20% of the original level. The  $^{106}\text{Ru}$  and the  $^{154}\text{Eu}$  distributions were similar, with greater than original concentrations near the bottom end of the original fuel location and lower concentrations, 50 to 90% of original, over the upper 60% of the original fuel location. These data indicate that some limited fuel collapse or meltdown had occurred, but that most of the fuel remained in a vertical column, as had been concluded from the in-cell radiation detector

measurements during the tests. The distributions of  $^{60}\text{Co}$  and  $^{125}\text{Sb}$  (see Figure 3.2) had been drastically altered. Very high concentrations of these two nuclides appeared 3 to 4 cm below the original fuel location, clearly identifying a large deposit of the Zircaloy cladding that contained the  $^{60}\text{Co}$ , an activation product, and a significant concentration of  $^{106}\text{Ru}$  as well.

In general, we believe that  $^{144}\text{Ce}$  is the best indicator of fuel location. Because of the long decay time for the fuel in test VI-6 (~12 y), however, the counting precision for  $^{144}\text{Ce}$  ( $T_{1/2} = 284$  d) was poor. Therefore, in test VI-6,  $^{154}\text{Eu}$  is believed to be the best indicator for the location of  $\text{UO}_2$  fuel. Since some  $^{154}\text{Eu}$  was found below the original fuel location, it appears that a small amount of  $\text{UO}_2$  either fell down as particles of fuel or was dissolved and carried down by the molten Zircaloy cladding.

As has been typical of these tests of high-burnup, long-decayed fuel,  $^{137}\text{Cs}$  and  $^{134}\text{Cs}$  were the dominant activities in almost all samples of released material and interfered with the analysis of less abundant fission products. The integral release behavior of krypton, as functions of time and temperature, is illustrated in Figure 3.3. The cesium release behaviors from the top and bottom regions of the fuel specimen, as indicated by the in-cell fuel monitors, are compared with this krypton release curve in Figure 3.4. This figure indicates that cesium release from the top of the specimen occurred somewhat earlier than from the bottom, suggesting a higher temperature at the top. The distributions of the cesium release to the TGTs (primarily vapor forms) and to the filters (primarily aerosol forms) are shown in Figure 3.5. These data were obtained from the NaI(Tl) detectors which measured  $^{137}\text{Cs}$  directly. The latter are believed to be more reliable than the fuel monitors that supplied the gross gamma data shown in Figure 3.4. These curves in Figures 3.3, 3.4, and 3.5 show that the maximum release rate occurred during the period of clad melting and rundown, at temperatures of 2050 to 2300 K (at 50 to 54 min), as was observed in test VI-5 in hydrogen.<sup>6</sup> During Test Phase B and the first 20 min of Test Phase C, the period of very low flow rate because of the steam leak, Kr and Cs release rates declined. When high steam flow was established

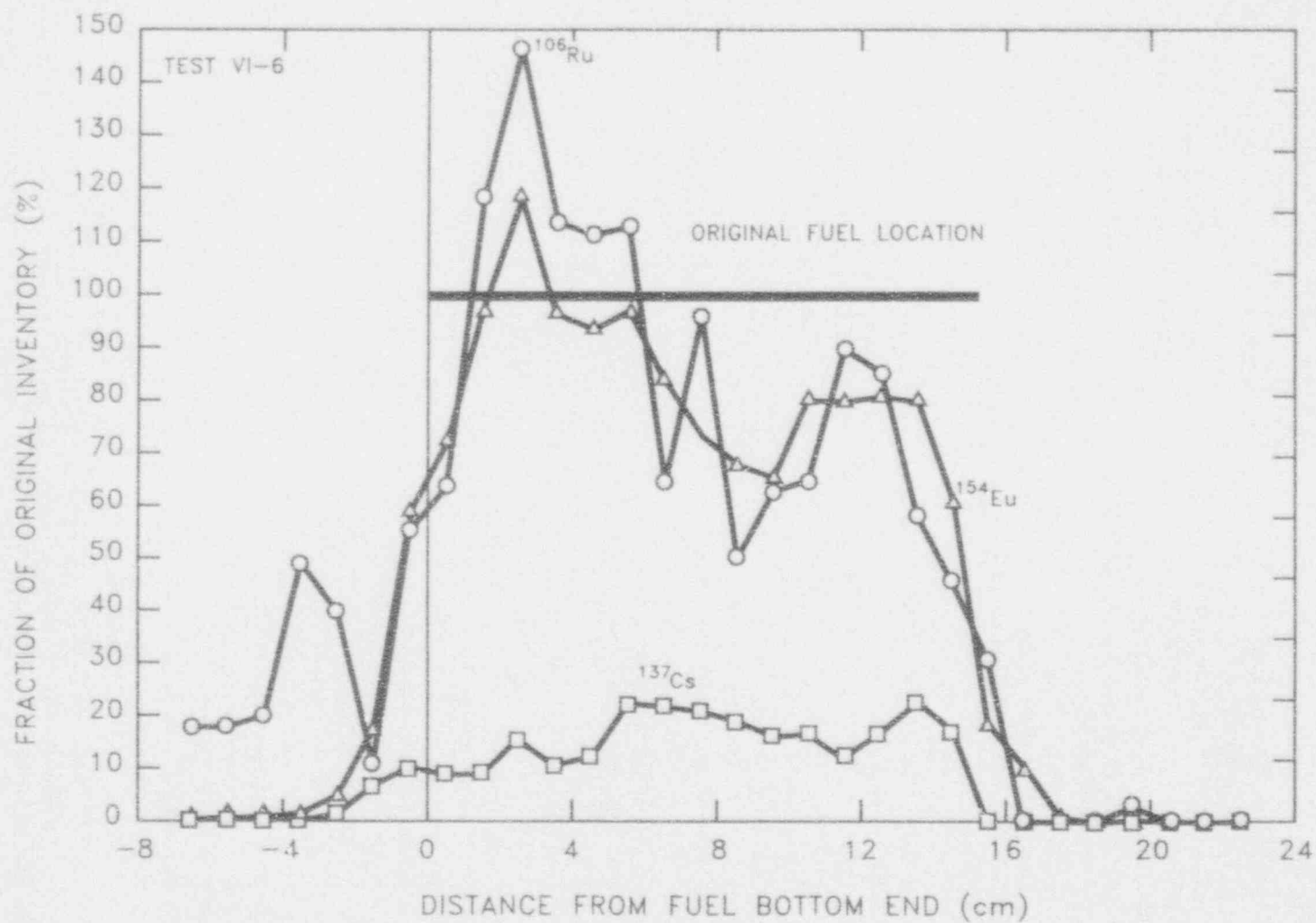


Figure 3.1 Distributions of fission product  $^{106}\text{Ru}$ ,  $^{137}\text{Cs}$ , and  $^{154}\text{Eu}$  in the fuel-furnace tube assembly after test VI-6

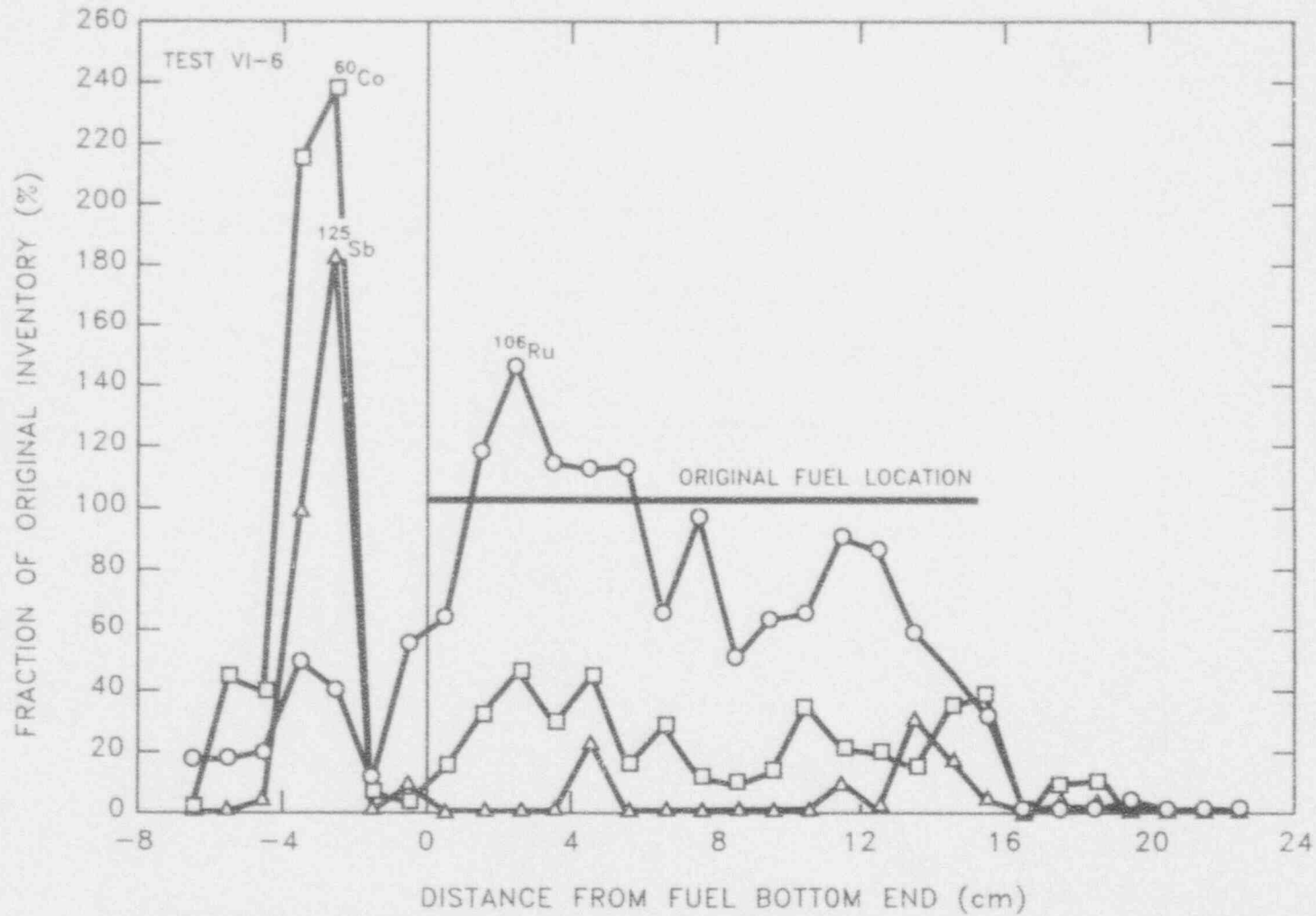


Figure 3.2 Distribution of  $^{106}\text{Ru}$ ,  $^{125}\text{Sb}$ , and  $^{60}\text{Co}$  in the fuel-furnace tube assembly after test VI-6



ORNL DWG 92A-720

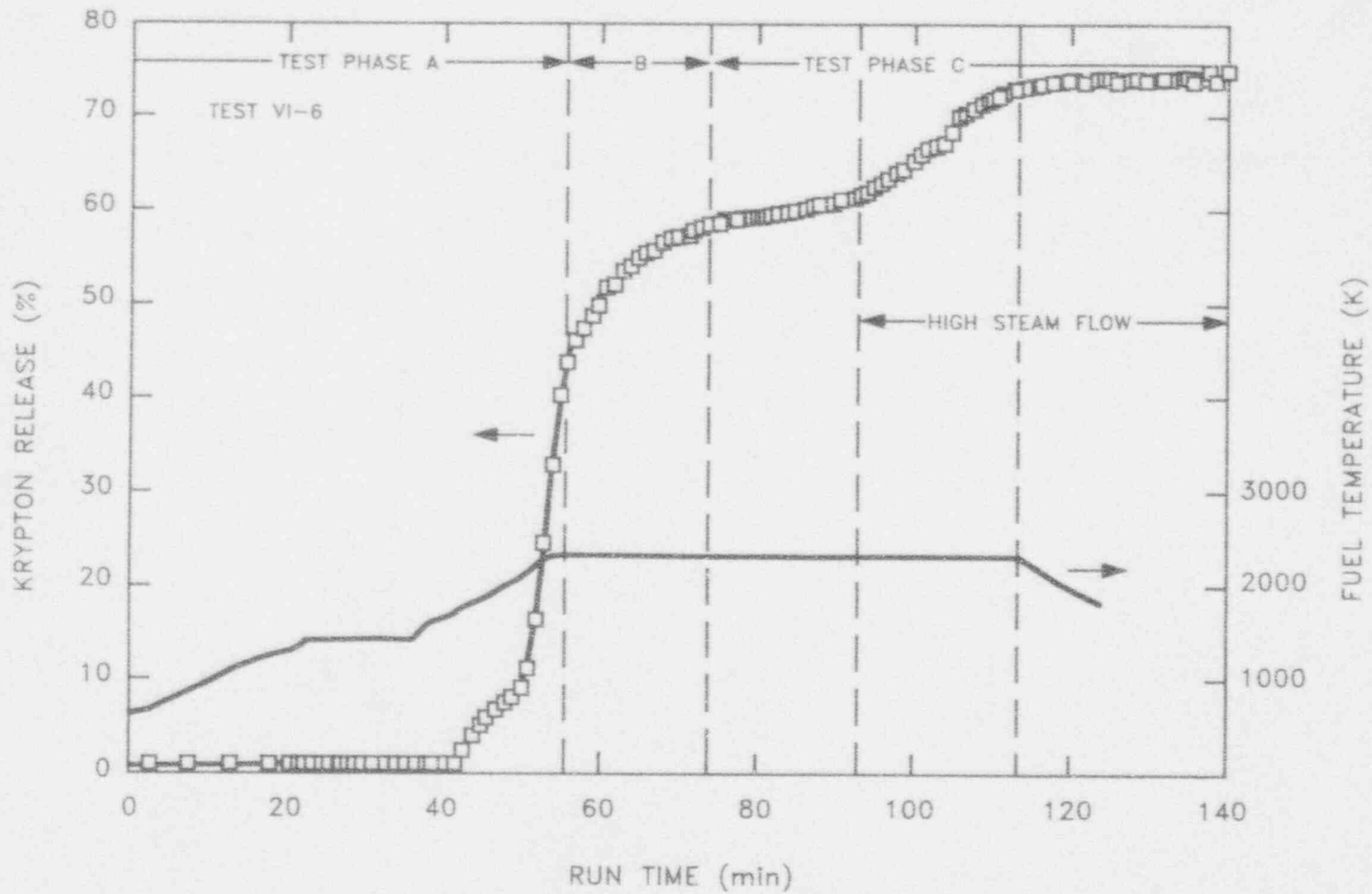


Figure 3.3 Release behavior of <sup>85</sup>Kr vs time and temperature in test VI-6

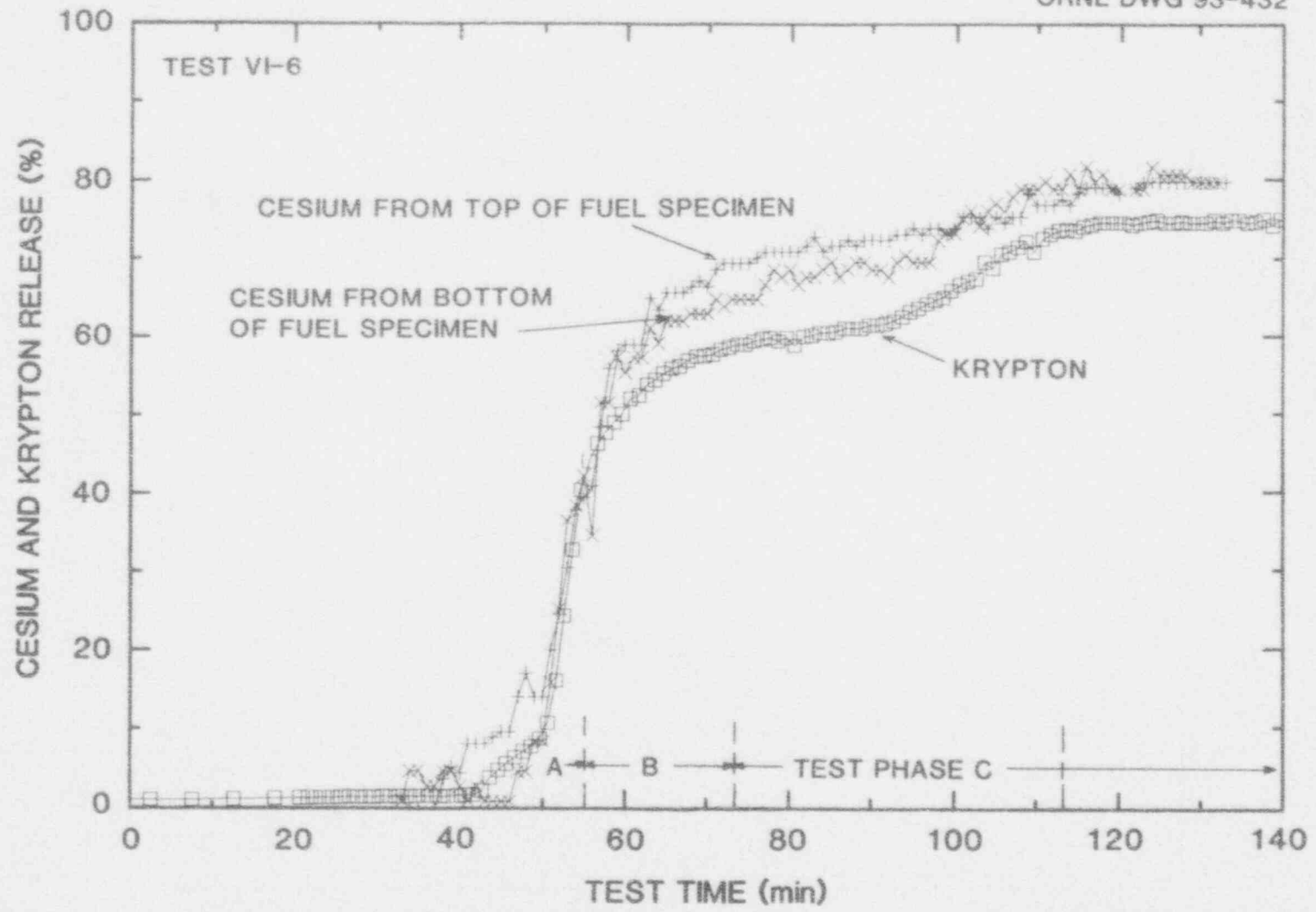


Figure 3.4 Release behavior of <sup>137</sup>Cs from fuel during test VI-6, as indicated by detectors monitoring top and bottom regions of the fuel specimen

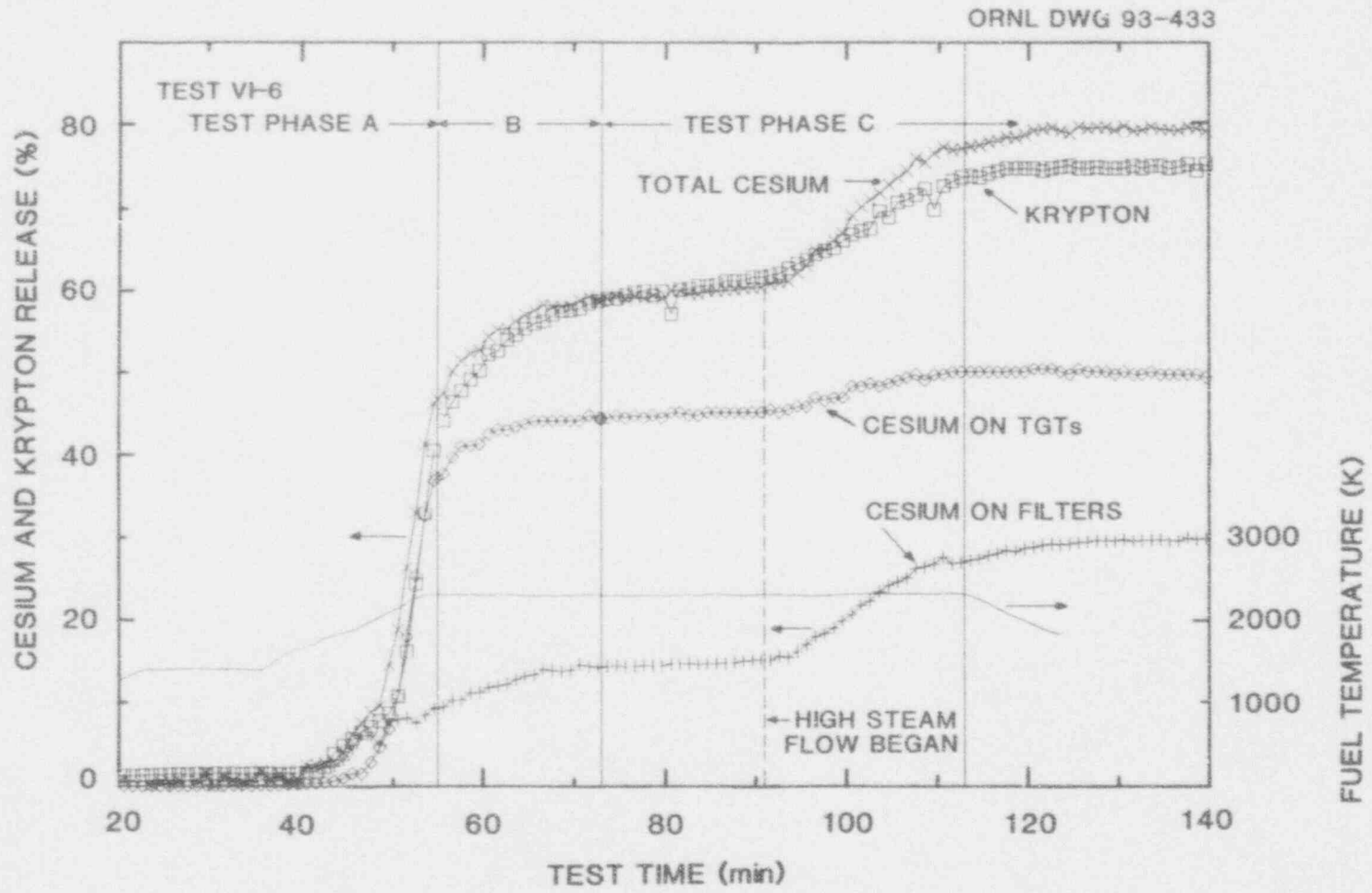


Figure 3.5 On-line distribution of released cesium forms, vapor to TGTs and aerosol filters, compared to krypton release behavior

across the fuel specimen, at a test time of 93 min, a rapid increase in release rates was observed, showing the effect of steam oxidation on the  $\text{UO}_2$ .

A summary of the fractional release results for Kr, Sb, Cs, and Eu, as determined by gamma spectrometry, and for  $^{129}\text{I}$ , as determined by neutron activation analysis, is presented in Table 3.1. Although no data for  $^{134}\text{Cs}$  are shown, the agreement with  $^{137}\text{Cs}$  was consistently good (within  $\pm 3\%$ ) at all locations. Since there is no apparent reason for a separation of the two Cs radionuclides, this is a good indication of the precision of the analyses. The distribution of cesium within the test apparatus is shown in detail in Table 3.2. An unusually large fraction,  $\sim 54.3\%$ , of the cesium released from the fuel was retained in the furnace in test VI-6. The fractional retention values for cesium within the furnaces for the six VI series tests are compared in Table 3.3. Except for test VI-4 (2440 K in hydrogen), which had a furnace retention fraction of 47.1%, only 4 to 11% of the released cesium was retained in any previous VI test. As observed in other tests, this suggests that cesium reacted with the  $\text{ZrO}_2$  ceramics to form some cesium compound, probably  $\text{Cs}_2\text{ZrO}_3$ , more efficiently under these conditions than in steam, or at different temperatures.<sup>13</sup>

The measured distributions for the released  $^{125}\text{Sb}$  and  $^{154}\text{Eu}$  within the test apparatus are shown in Table 3.4. Although these nuclides are of relatively low yield and are not among the most hazardous, they have intermediate half-lives and strong gamma rays, which make them easily detected. Because previous release results showed moderate Eu release in hydrogen but almost none in steam, most of the europium release in test VI-6 (13.7%) is believed to have occurred during Test Phase A (in hydrogen). Very little europium, which is relatively involatile under oxidizing conditions, has been released in tests in steam, but 13.4% was released in test VI-4 at 2440 K in hydrogen. As shown in Table 3.3, significant fractions (6.7 and 55%, respectively) of the released Sb and Eu were deposited on ceramic surfaces in the outlet region of the furnace, where temperatures were believed to be 1500 to 2200 K during the test.

In order to calculate the release of cesium as a function of time, it is necessary to allocate the amount of cesium collected on the furnace components to the A,

B, and C collection periods. The simplest method is to assume that the cesium deposited in the furnace was released from the fuel at the same rate as the cesium that was deposited in the A, B, and C collection systems. This is the method that was used with the ST-1 test, but it gave erroneous results for test VI-6. When this method was tried, the resulting release rates did not agree with those measured by the radiation detectors that were directed at the fuel rod itself, and it required unrealistic changes in efficiency for the radiation detector monitoring the thermal gradient tube and the top of the furnace.

The following procedure was used to calculate the amounts of vapor-form cesium and aerosol-associated cesium and the times that they were released from the fuel.

- (1) All of the cesium deposited on the TGTs and on the  $\text{ZrO}_2$  plugs at the top of the furnace was assumed to have been in a vapor form before condensation or reaction with the  $\text{ZrO}_2$ .
- (2) All of the cesium collected on the filters and filter inlet lines was assumed to be aerosol associated.
- (3) The amount of cesium deposited in the furnace inlet and exit regions was assumed to have a vapor/aerosol form ratio the same as the vapor/aerosol ratio calculated from the total amounts in steps 1 and 2.
- (4) The amount of aerosol-associated cesium calculated in step 3 was distributed to time periods A, B, and C in direct proportion to the amounts calculated in step 2.
- (5) The amount of vapor-form cesium calculated for the furnace deposits in step 3 was allocated to time periods A, B, and C according to the radiation detector that monitored cesium deposition in the TGTs and the top of the furnace each minute during the test.

The results of this calculation are shown in Table 3.5 and Figure 3.5. The on-line radiation detectors are the NaI crystal type which permitted measurement of both  $^{134}\text{Cs}$  and  $^{137}\text{Cs}$ . The  $^{134}\text{Cs}$  data were used in preference to the  $^{137}\text{Cs}$  data so that it was not necessary to

## Results

Table 3.1 Summary of fission product release data for test VI-6

Location	Operating time at T >2000 K (min)	Fraction of fission product inventory found (%)*				
		<sup>85</sup> Kr	<sup>125</sup> Sb	<sup>129</sup> I	<sup>137</sup> Cs	<sup>154</sup> Eu
Furnace components	72	0	20.5	23.1	43.5	13.4
Collection Train A:	6					
TGT A			0.0	3.50	8.34	0.0
Filters			0.0	14.7	5.37	0.04
Total Train A		42.0	0.0	18.2	13.71	0.04
Collection Train B:	18					
TGT B			0.0	1.84	2.57	0.0
Filters			0.0	2.04	2.78	0.001
Total Train B		16.9	0.0	3.88	5.35	0.001
Collection Train C	48					
TGT C			8.35	5.67	8.91	0.028
Filters			34.64	16.1	8.59	0.167
Total Train C		16.4	42.99	21.8	17.50	0.195
Total for test	72	75.3	63.5	66.9	80.1	13.7

\*Inventories based on pretest gamma analysis of the fuel and ORIGEN2 calculations.

Table 3.2 Cesium release and distribution data for test VI-6

Location	Approximate temperature (K)	Cesium found at each location*		
		<sup>137</sup> Cs (mCi)	Total Cs (mg)	(% of inventory)
<b>Furnace components</b>				
Inlet region	500—1600	208.0	5.99	2.742
First ZrO <sub>2</sub> plug	~ 2100	2.2	0.06	0.029
Second ZrO <sub>2</sub> plug	~ 1700	1160.0	33.43	15.291
Exit region	500—1600	1931.0	55.65	25.455
Total		3301.2	95.14	43.52
<b>Train A</b>				
TGT A	470—1000	632.3	18.22	8.335
TGT — filter line	430	72.1	2.08	0.950
First prefilter	405	311.0	8.96	4.100
Second prefilter	405	22.8	0.66	0.301
HEPA filters	405	2.2	0.06	0.029
Total		1040.4	29.98	13.71
<b>Train B</b>				
TGT B	470—1070	194.7	5.61	2.567
TGT — filter line	430	23.4	0.67	0.308
First prefilter	410	152.0	4.38	2.004
Second prefilter	410	33.4	0.96	0.440
HEPA filters	410	2.3	0.07	0.030
Total		405.8	11.70	5.35
<b>Train C</b>				
TGT C	407—1010	675.5	19.47	8.905
TGT — filter line	430	62.4	1.80	0.823
First prefilter	410	582.5	16.79	7.679
Second prefilter	410	6.8	0.20	0.090
HEPA filters	410	0.6	0.02	0.008
Total		1327.8	38.27	17.50
Total released from fuel		6075	175	80.08
Total in fuel (after test)		1511	43.55	19.92

\*Inventory based on measured data: 7586 mCi <sup>137</sup>Cs on July 1, 1991; 0.02882 mg Cs/mCi based on ORIGEN2.

## Results

Table 3.3 Retention in furnace of cesium released from fuel in VI tests

	Test No.					
	VI-1	VI-2	VI-3	VI-4*	VI-5	VI-6
Test temperature (K)	2020/2300	2300	2000/2700	2440	2000/2720	2310
Test atmosphere	Steam	Steam	Steam	H <sub>2</sub>	H <sub>2</sub>	H <sub>2</sub> /steam
Released from fuel (% of fuel inventory)	63.1	67.2	99.9	96.1	100	80.1
Retained in furnace (% of fuel inventory)	4.00	2.87	10.6	45.9	7.63	43.5
Retained in furnace (% of release from fuel)	6.34	4.27	10.6	47.1	7.63	54.3

\*The upper half of the furnace was intentionally cooled in test VI-4 to duplicate the conditions of SNL test ST-1.

Table 3.4 Fractional release and distribution of antimony and europium in test VI-6<sup>c</sup>

Location	<sup>125</sup> Sb			<sup>154</sup> Eu		
	(mCi)	(% of inventory)	(% of released)	(mCi)	(% of inventory)	(% of released)
<b>Furnace components</b>						
First ZrO <sub>2</sub> plug	0.236	0.796	1.255	20.014	12.635	92.416
Second ZrO <sub>2</sub> plug	3.670	12.386	19.511	1.103	0.696	5.091
Exit region	2.170	7.324	11.536	0.159	0.100	0.734
Furnace total	6.076	20.506	32.302	21.275	13.431	98.241
<b>Train A</b>						
TGT A	0.000	0.000	0.000	0.000	0.000	0.000
TGT — filter line	0.000	0.000	0.000	0.028	0.018	0.130
First prefilter	0.000	0.000	0.000	0.039	0.025	0.180
Second prefilter	0.000	0.000	0.000	0.000	0.000	0.000
HEPA filters	0.000	0.000	0.000	0.000	0.000	0.000
Train A total	0.000	0.000	0.000	0.067	0.042	0.311
<b>Train B</b>						
TGT B	0.000	0.000	0.000	0.000	0.000	0.000
TGT — filter line	0.000	0.000	0.000	0.002	0.001	0.000
First prefilter	0.000	0.000	0.000	0.000	0.000	0.000
Second prefilter	0.000	0.000	0.000	0.000	0.000	0.000
HEPA filters	0.000	0.000	0.000	0.000	0.000	0.000
Train B total	0.000	0.000	0.000	0.002	0.001	0.001
<b>Train C</b>						
TGT C	2.474	8.350	13.153	0.046	0.029	0.212
TGT C — filter line	0.997	3.365	5.300	0.030	0.019	0.138
First prefilter	9.220	31.117	49.016	0.230	0.145	1.061
Second prefilter	0.042	0.142	0.223	0.005	0.003	0.021
HEPA filters	0.005	0.017	0.027	0.000	0.000	0.000
Train C total	12.74	42.990	67.719	0.310	0.196	1.432
Total released from fuel	18.81	63.50	100.02	21.655	13.671	99.98
Total in fuel (after test)	10.82	36.52		149.0	86.33	

<sup>c</sup>Inventories based on measured data: 29.63 mCi <sup>125</sup>Sb and 172.6 mCi <sup>154</sup>Eu.



Table 3.5 Physical form of released cesium

Collection period	Amount in designated form (% of inventory)		
	Vapor	Aerosol	Total
A	37.4	9.5	46.9
B	7.1	5.0	12.1
C	5.8	15.3	21.1
Total A+B+C	50.3	29.8	80.1

correct for the time delay caused by the  $^{137}\text{m}\text{Ba}$  gamma being emitted from the  $^{137}\text{Ba}$  daughter. Good agreement is evident between Figures 3.5 and 3.4, and between cesium and krypton in Figure 3.5.

### 3.2 Analysis for Iodine

Since iodine has no long-lived, gamma-emitting nuclides, analytical methods other than gamma spectrometry must be used to determine its behavior. Neutron activation of  $^{129}\text{I}$  to  $^{130}\text{I}$ , which has abundant, easily measured gamma rays, is a proven and sensitive technique. Because the normally occurring iodine forms dissolve readily in basic solutions to form stable iodides, the collector components from this test were leached to remove this iodine for analysis.

The results of iodine analysis are summarized in Tables 3.1 and 3.6. As indicated, the total releases of I and Cs were significantly different. Some 34% of the released  $^{129}\text{I}$ , compared to 54% of the released cesium, was deposited in the furnace. In addition, a larger fraction of the iodine was collected on the filters (75% vs 25% on TGTs), compared to nearly equal fractions (46% on filters vs 54% on TGTs) for cesium, as shown in Table 3.7.

Some iodine forms (organic iodides, elemental iodine, or hydrogen iodide) may pass through the TGTs, penetrate the filters, and adsorb onto the heated charcoal in the filter packages. For this reason, the charcoal cartridges, which back up the filters, were analyzed for  $^{129}\text{I}$  by direct activation also. The results of these analyses are shown in Table 3.8. The fraction of the released iodine that was collected on the

charcoal (5.1%) was higher in test VI-6 than in any previous test, which normally averaged <0.5%.

A possible source of the volatile iodine is radiation decomposition of an iodine species collected as particulate material on the glass wool and HEPA filters. Because the activated charcoal cartridges are part of the filter pack assembly and are located close to the highly radioactive filters, they would have received a relatively high radiation dose rate. In test VI-6, the filter/charcoal assembly remained sealed for 5 months after the test, a longer period than in most tests. This extended period of exposure possibly resulted in some decomposition of CsI, with the released iodine being sorbed on the nearby charcoal.

### 3.3 Thermal Gradient Tube Deposits

The three TGT liners were made by rolling 0.002-in.-thick stainless steel foil into tubes. Except for being annealed in He-4%  $\text{H}_2$  to aid forming, the surfaces of the liners were in the as-received condition. These liners were removed from the surrounding Inconel TGTs and examined. During the test, each of the 36-cm-long TGT liners had been subjected to maximum temperatures of  $\sim 850^\circ\text{C}$  (1125 K) at the inlet end. The TGT temperatures declined approximately linearly to  $\sim 150^\circ\text{C}$  at the exit end. All three liners showed evidence of external corrosion over the first few centimeters at the inlet ends, but the liner from TGT A (through which the furnace exit gas flowed during heatup and for the first 2 min at 2300 K) was much more corroded than Liners B and C, from Phases B and C later in the test. This severe corrosion, to the extent that the first  $\sim 5$  cm of Liner A

Table 3.6 Iodine release and distribution data for test VI-6

Location	Approximate temperature (K)	<sup>129</sup> I found at each location*	
		<sup>129</sup> I (μg)	Percent of inventory
Furnace components			
Inlet region	500—1600	1	0.01
First ZrO <sub>2</sub> plug	~ 2100	0	0
Second ZrO <sub>2</sub> plug	~ 1700	0	0
Exit region ceramics	800—1600	400	3.11
Exit flange	350—1100	2574	19.99
Total		2975	23.11
Train A			
TGT A	470—1000	451	3.50
TGT — filter line	430	245	1.90
First prefilter	405	1301	10.11
Second prefilter	405	0	0
HEPA filters	405	0	0
Charcoal	405	339	2.63
Total		2337	18.15
Train B			
TGT B	470—1070	237	1.84
TGT — filter line	430	18	0.14
First prefilter	410	180	1.40
Second prefilter	410	0	0
HEPA filters	410	0	0
Charcoal	410	64	0.50
Total		500	3.88
Train C			
TGT C	407—1010	730	5.67
TGT — filter line	430	125	0.97
First prefilter	410	1516	11.78
Second prefilter	410	0	0
HEPA filters	410	0	0
Charcoal	410	428	3.33
Total		2799	21.74
Total released from fuel		8611	66.89

\*Inventory based on ORIGEN2 calculation: 12.87 mg <sup>129</sup>I and 15.92 total iodine in fuel.

## Results

Table 3.7 Comparison of physical forms of iodine and cesium released to collection trains

Collection period	Fraction in designated form (% of element released from furnace)*					
	Vapor		Aerosol		Total	
	I	Cs	I	Cs	I	Cs
A	8.0	22.8	33.6	14.7	41.6	37.5
B	4.2	7.0	4.7	7.6	8.9	14.6
C	13.0	24.3	36.8	23.5	49.8	47.8
Total A+B+C	25.2	54.1	75.1	45.8	100.3	99.9

\*Based on total inventory in the fuel, 43.8% of the iodine and 36.6% of the cesium were released from the furnace.

Table 3.8 Volatile iodine in test VI-6

Sample No.	Volatile iodine*	
	Mass ( $\mu\text{g}$ )	Percent of released†
AC1	339	2.1
AC2	0.1	0.0
AC3	ND**	0.0
BC1	64	0.4
BC2	ND	0.0
BC3	ND	0.0
CC1	428	2.6
CC2	0.1	0.0
CC3	ND	0.0
Totals	831	5.1

\*As determined by measurements of  $^{129}\text{I}$ .

\*\*ND = Not Detected.

† Assumes that total iodine release is the same as the cesium release, 80.09% of total inventory.

disintegrated during removal, indicated that the material released from the furnace during Phase A was more corrosive than that released later in the test. Upon opening the liners, the internal deposits in Liner A appeared to be uniformly distributed and heavier than those in Liner B, but not as heavy as those in Liner C.

The collection of cesium on the stainless steel TGT liners was monitored during the test by counting the  $^{134}\text{Cs}$  and  $^{137}\text{Cs}$  continuously. The final  $^{137}\text{Cs}$  profiles, as well as the temperature profile along the TGTs, are shown in Figure 3.6. Although small amounts of  $^{125}\text{Sb}$  (in TGT C) and  $^{154}\text{Eu}$  (in TGTs A and C) were present, as measured by long counts and shown in Table 3.4, the profiles could not be measured concurrently with the  $^{137}\text{Cs}$  profile. The fact that most of the cesium released during Test Phase B was in vapor form, as indicated by its deposition on TGT Liner B rather than on Filter B, confirms that little steam was present during this period. (Previous tests have shown that in a steam atmosphere, ~70% of the released cesium is transported as aerosols, which are collected primarily on the filters.<sup>7</sup>) Only when full steam flow through the furnace was established (at 93 min) did most of the cesium pass through the TGTs to be collected on the filters, presumably as oxide or hydroxide forms.

### 3.4 Masses of Deposits in TGTS and on Filters

The filters and TGT liners were weighed before and after the test to determine the mass of material collected. Most of the material deposited in the TGT liners is believed to be a result of vapor condensation, and the material deposited on the filters probably was transported primarily as aerosol. Immediately after disassembly of the filter packages, the filters were inspected and packaged for weighing. Although the prefilters exhibited light deposits, no deposits were visible and no weight changes were observed for the HEPA filters, indicating efficient collection of the aerosols by the prefilters.

The masses of material collected at the various locations are listed in Table 3.9 and illustrated in Figure 3.7. Because of the disintegration of the inlet end of Liner A, as mentioned above, an accurate weight was impossible. Based on the relative

appearances of the test VI-6 liners, and on measurements from other tests, we estimated that Liner A contained ~100 mg of deposits.

As would be expected, the greatest mass was collected during Phase C, the longest collection period, and also the period of steam flow. (Previous tests, such as VI-3 and VI-5, have shown that mass releases are much greater in steam than in hydrogen.) The total mass collected (0.573 g) was much less than in the all-steam atmosphere test VI-2 (1.134 g) at the same temperature and time. Since 68% of the released mass (0.391 g) was found in Train C, the period with steam atmosphere, test VI-6 behavior was consistent with earlier tests.

### 3.5 ICP-ES Analyses

Samples of the acidic leach solutions from the TGT liners and the filters were submitted for inductively coupled plasma-emission spectrometry (ICP-ES) analyses for non-gamma-emitting elements. This technique is well suited for measuring several of the fission product elements, primarily cations, and uranium. Unfortunately, it is not useful for iodine analysis. Because of the high levels of radiocesium in most of the samples, large dilutions, which reduced the precision of the measurements, have been required to avoid excess radiation dose to the analyst.

As would be expected, major release fractions of all these elements were retained in the outlet end of the furnace, where the time (Test Phase A, B, or C) of release and/or deposition cannot be determined. Furthermore, the largest fractions of these four elements that were released to the collection trains were found in Train C, as shown in Table 3.10. The larger fractions in Train C are consistent with the steam atmosphere during that period, which tended to accelerate release by oxidizing the  $\text{UO}_2$ , and the longer period of operation, 40 min as opposed to 2 min and 18 min at 2300 K for Trains A and B, respectively.

Because of their well-known sensitivity to the effects of oxidizing conditions, most of the release of Mo and Te is believed to have occurred during the latter part of Phase C, after the cladding had been oxidized by the steam. The observed behavior of these four less-volatile fission product elements is in general

ORNL DWG 92A-434

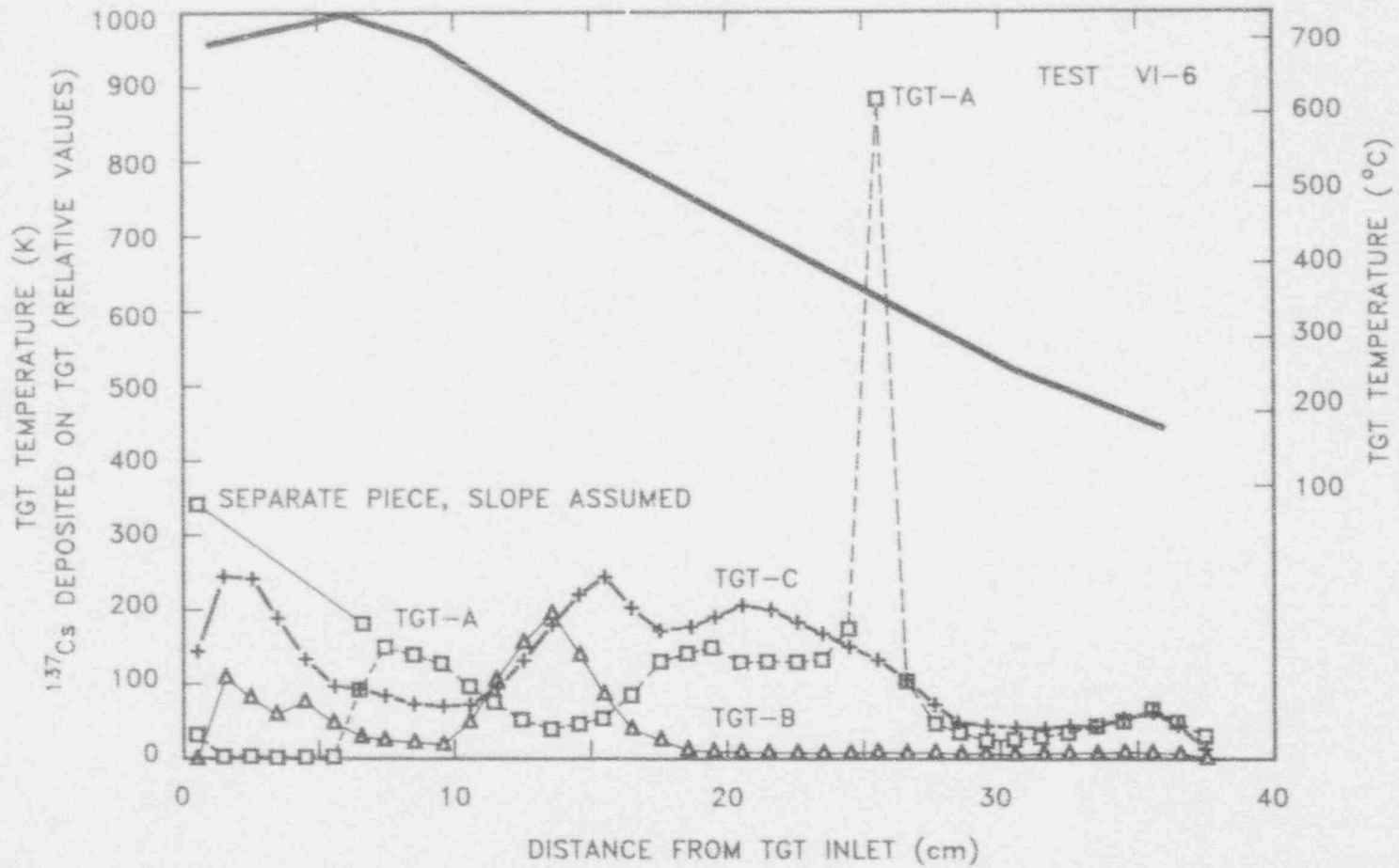


Figure 3.6 Distributions of <sup>137</sup>Cs along thermal gradient tubes A, B, and C in test VI-6. Note temperature profile also

Table 3.9 Vapor and aerosol deposits in test VI-6

	Weight of deposits (g)*			
	Train A	Train B	Train C	Total
Thermal gradient tube (TGT)	0.100**	0.031	0.161	0.292
Filters				
Prefilter 1 <sup>+</sup>	0.036	0.015	0.230	0.281
Prefilter 2	0.000	0.000	0.000	0.000
HEPAs	0.000	0.000	0.000	0.000
Total filters	0.036	0.015	0.230	0.281
Total TGT and filters	0.136	0.046	0.391	0.573

\*Precision =  $\pm 0.003$  g.

\*\*Estimated value; inlet end of TGT A was corroded and disintegrated.

+Includes estimated mass of deposits in connecting tubes, based on <sup>137</sup>Cs data.

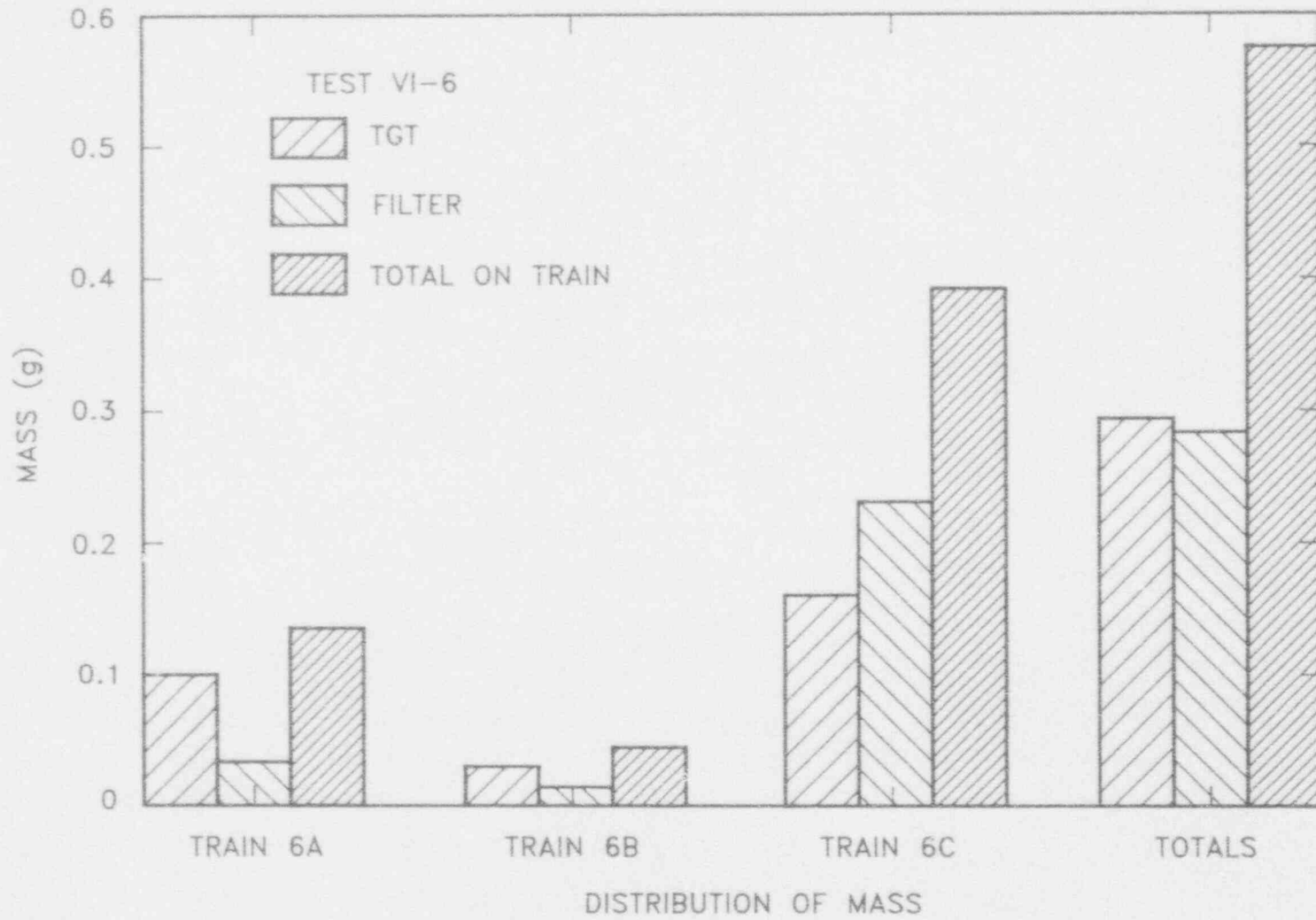


Figure 3.7 Mass distribution to the collection system of material released during test VI-6

Table 3.10 Test VI-6 release data for less-volatile fission products

Location	Time fuel at 2300 K (min)	Release (% of inventory)			
		Sr	Mo	Te	Ba
Furnace	60	5.50	12.2	40.7	29.0
Train A	2	0.087	0.015	1.80	1.10
Train B	18	0.063	0.008	1.43	0.817
Train C	40	0.171	0.40	19.5	1.45
Totals		5.82	12.6	63.4	32.4

agreement with the CORSOR model and with other experimental data.<sup>14</sup>

### 3.6 Modeling of Volatile Fission Product Release

Because the <sup>85</sup>Kr, <sup>134</sup>Cs, and <sup>137</sup>Cs were collected and measured on-line at 1-min intervals during the test, calculation of the minute-by-minute release rates was readily accomplished. As in previous tests, the release behaviors of Kr and Cs were similar, including the transition period from hydrogen (reducing) to steam (oxidizing) atmospheres.

The on-line data for Kr and Cs were used to calculate the minute-by-minute diffusion coefficients during test VI-6, and the <sup>85</sup>Kr diffusion coefficients are plotted vs temperature in Figure 3.8. Good agreement with a

curve representing the ORNL Diffusion Model is apparent, and the agreement of Cs data with the model was comparable. This model, which uses data from previous tests, most of which were in steam, and includes the effects of grain size and burnup, has been described elsewhere.<sup>7</sup> As may be seen in Figure 3.8, the values from test VI-6 fall somewhat above the curve at the lowest temperatures (<1500 K). This release is believed to result from a combination of poor counting statistics and surface desorption of nuclides released and adsorbed during irradiation, rather than from diffusion from the fuel matrix. The vertical cluster of points at 2300 K reflects the decline in release rate with time, as a result of source depletion, at the constant test temperature. A plot of the same diffusion coefficients for <sup>85</sup>Kr as a function of time is presented in Figure 3.9. The decline in diffusion coefficient during the period of low steam flow (~55 to 93 min) and the increase in diffusion coefficient with increased steam flow are apparent in this figure.





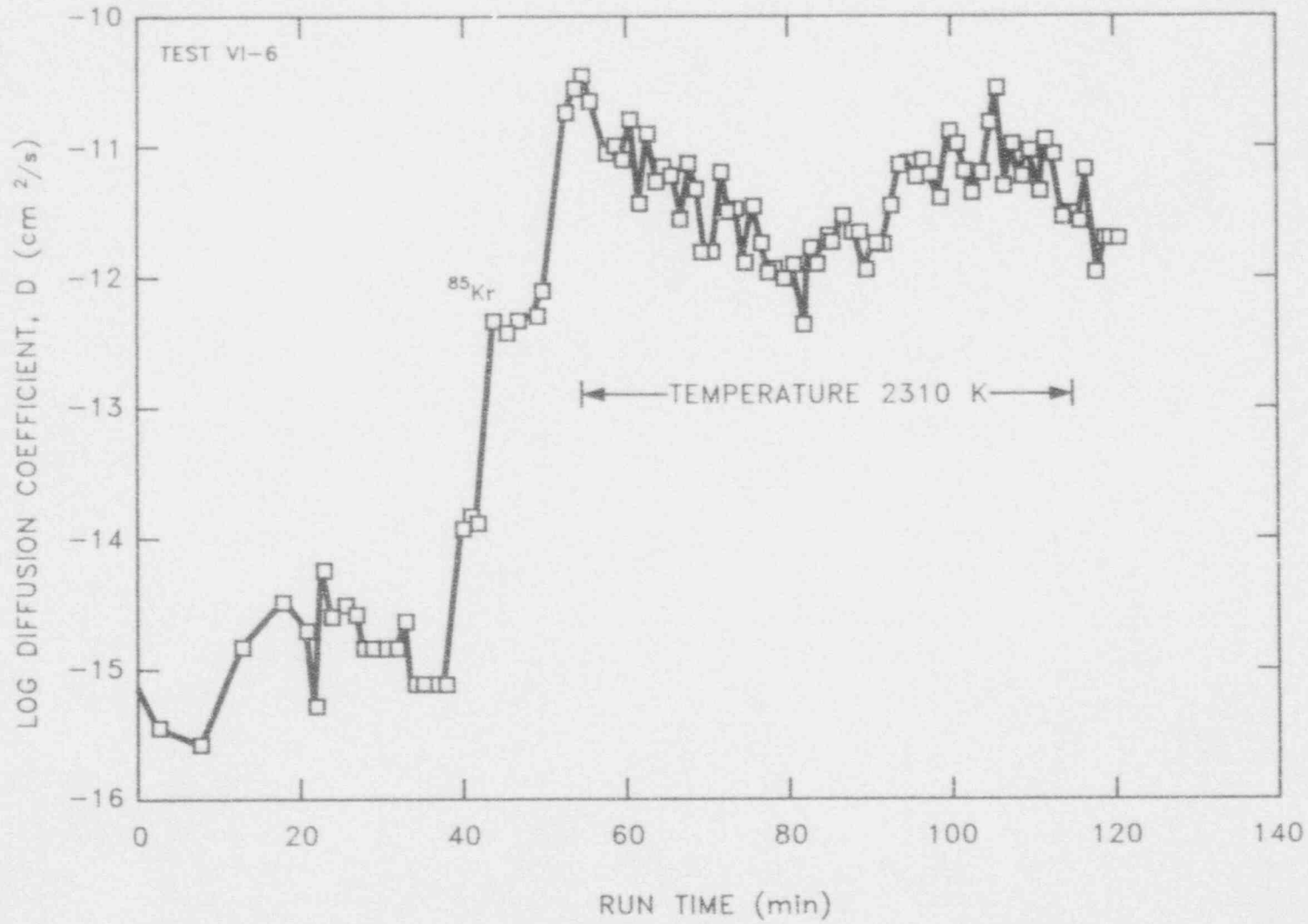
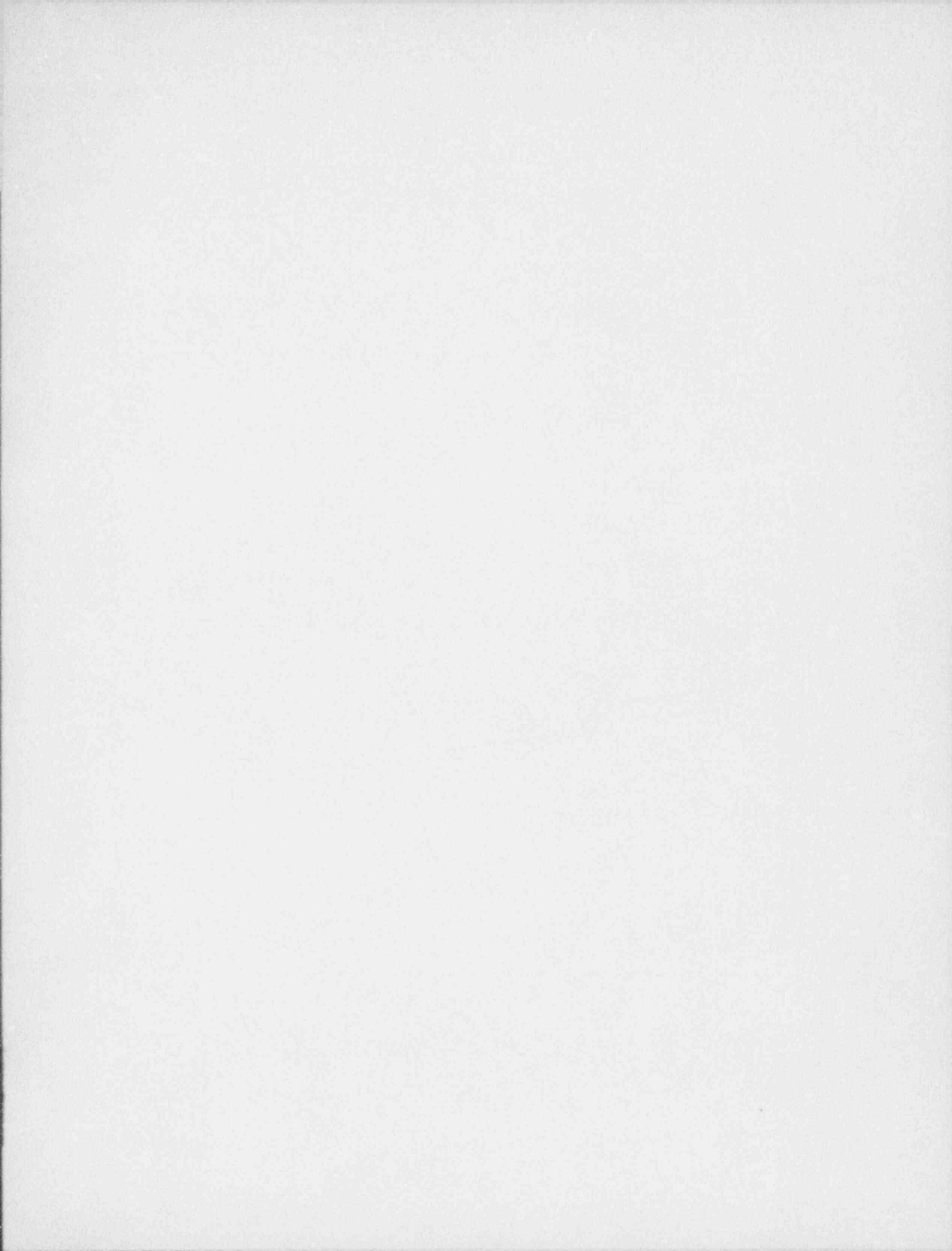


Figure 3.9 Diffusion coefficients for  $^{85}\text{Kr}$  at constant test temperature (2310 K) in test VI-6



## 4 Comparison of Release Data with Previous Results

The fission product release data from this test (VI-6) have been compared with the results from earlier experiments and also with results from an earlier comprehensive NRC review of all relevant fission product release data, which was the basis for the CORSOR model.<sup>15</sup> Because test VI-6 was essentially identical to test VI-2 except for the change in atmosphere, we were particularly interested in comparing the results from these two tests.

The integral release data for nine fission product elements from test VI-6 are compared with results of previous tests of BR3 fuel (VI-2, VI-3, VI-4, and VI-5) in Table 4.1. The VI-6 data, with test phase differentiation, are plotted in Figure 4.1. For Figure 4.1, the release of furnace-deposited material was assumed to be at the same relative rate as material collected in systems A, B, and C. The fractional releases of krypton and cesium were always similar, except for the lower krypton value for test VI-2, where some of the gas was known to have been lost, and exhibited a general increase with test temperature, reaching ~100% at 2700 K. The release behavior of iodine is

believed to be similar to that of krypton and cesium; the somewhat lower values for iodine shown in Table 4.1 can be explained by the problems of thorough sampling and neutron activation analysis. No significant influence of the reactive atmospheres, steam and hydrogen, on the release of these highly volatile elements was apparent.

With regard to atmospheric effects on the less-volatile species, the recent data supported the conclusions drawn from earlier results.<sup>16,17</sup> The release behaviors of Sb, Sr, Mo, Te, Ba, and Eu, on the other hand, showed a clear influence of the reactive atmospheres, and these atmospheric effects became more exaggerated at the highest temperature, 2700 K. Much higher release of Sb and Mo was observed in steam, whereas Ba, Sr, and Eu releases were higher in hydrogen. The data for Te appear inconsistent; incomplete sampling and analysis, as well as some uncertainties about the oxidation conditions, are believed to be the main problems in interpreting Te behavior. In conclusion, the behaviors of these elements in test VI-6 were found to be generally consistent with their chemical characteristics.

Comparison

Table 4.1 Comparison of fission product release data for VI tests

	Test No.				
	VI-2	VI-3	VI-4	VI-5	VI-6
<b>Test conditions</b>					
Test temperature (K)	230	2000/2700*	2400	2015/2740*	2310
Time at temp. (min)	60	20/20	20	20/20	60
Atmosphere**	Steam	Steam	Hydrogen	Hydrogen	Hydrogen/steam
<b>Fission product release</b>					
	(% Release from fuel)				
<sup>85</sup> Kr	>31	100	94	100	75
<sup>125</sup> Sb	68	99	6.4	18	64
<sup>129</sup> I	40	69	87	++	67
<sup>137</sup> Cs	67	100	96	100	80
Sr	ND†	2.7	++	34	5.8
Mo	86	77	7	2.3	13
Te	>50	100	<46	82	63
Ba	19	30	27	75	32
<sup>154</sup> Eu	0	~0.01	19	57	14

\*Tests VI-3 and VI-5 were conducted in two phases at two different temperatures.

\*\*In all tests, the reactive atmosphere was mixed with helium.

+ND = Not Detected.

++ Analysis incomplete.

†Extrapolated from limited data.

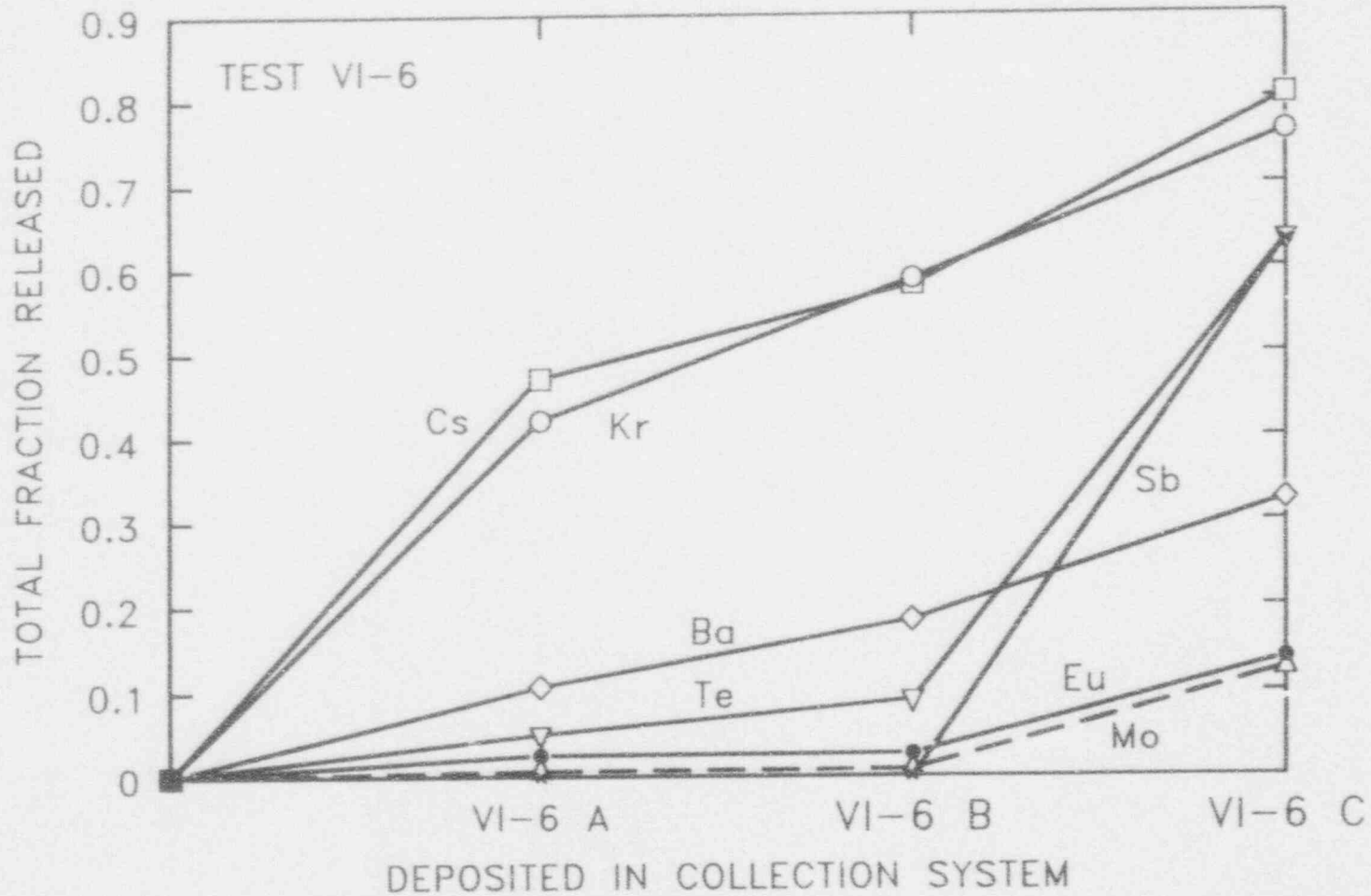


Figure 4.1 Total release fractions for Kr, Cs, Ba, Te, Sb, Eu, and Mo during the three phases of test VI-6



## 5 Summary and Conclusions

In view of the preliminary nature of this report and the fact that some important analyses/results have not yet been obtained, a thorough interpretation of the results of test VI-6 is not possible at this time. However, several significant observations are appropriate.

- (1) This was the second test at 2300 K for 60 min and the first test in which the atmosphere was changed from hydrogen to steam in mid-test. With the exception of the delay in establishing design steam flow through the furnace after hydrogen flow was stopped, the test was conducted as planned. Examination showed that the Zircaloy cladding had melted during the heatup in hydrogen and that only minimal collapse or run-down of the  $UO_2$  fuel had occurred.
- (2) The release values for many of the fission products were determined for the specific conditions of this test. The integral release values were 75% for Kr, 80% for Cs, 67% for I, 64% for Sb, 63% for Te, 32% for Ba, 5.8% for Sr, 13% for Mo, and 14% for Eu. Comparison of these release values with the results from previous tests showed generally consistent behavior of the fission products. The fractional release measurements for iodine will be completed and reported later.
- (3) Compared to previous tests, a larger fraction of the released fission products (32% of the Sb, 54% of the Cs, and 98% of the Eu) deposited on the  $ZrO_2$  ceramics in the outlet end of the furnace.
- (4) The total mass of deposits collected on the TGTs and the filters (0.57 g) was only 51% of that collected in test VI-2, which experienced the same temperature-time history. Most of this release occurred during Test Phase C, confirming previous observations of much higher mass release rates in steam than in hydrogen.
- (5) Approximately 5.1% of the released iodine was collected on the charcoal filter cartridges, indicating it had been in a volatile form —  $I_2$ ,  $I_2O_4$ , and/or  $CH_3I$ . This relatively high fraction is believed to result from radiation decomposition of more stable forms, such as CsI.
- (6) As in all previous tests, the release behaviors of the volatile species (Kr, I, and Cs) were very similar in test VI-6. In addition, the diffusion coefficients for Kr and Cs calculated from on-line release data were in good agreement with the ORNL Diffusion Model.
- (7) The fractional releases of several less-volatile fission product elements were found to be significant, varying from 5.8% for Sr to 63% for Te.



## 6 References

1. Osborne, M. F., J. L. Collins, and R. A. Lorenz, "Experimental Studies of Fission Product Release from Commercial LWR Fuel Under Accident Conditions," *Nucl. Technol.* 78(2):157-69, August 1987.
2. Osborne, M. F., J. L. Collins, R. A. Lorenz, J. R. Travis, C. S. Webster, and T. Yamashita, "Data Summary Report for Fission Product Release Test VI-1," NUREG/CR-5339 (ORNL/TM-11104), Oak Ridge National Laboratory, June 1989.
3. Osborne, M. F., J. L. Collins, R. A. Lorenz, J. R. Travis, and C. S. Webster, "Data Summary Report for Fission Product Release Test VI-2," NUREG/CR-5340 (ORNL/TM-11105), September 1989.
4. Osborne, M. F., J. L. Collins, R. A. Lorenz, J. R. Travis, C. S. Webster, S. R. Daish, H. K. Lee, T. Nakamura, and Y.-C. Tong, "Highlights Report for Fission Product Release Test VI-3," draft letter report to SFD Partners, July 1987.
5. Osborne, M. F., R. A. Lorenz, J. L. Collins, J. R. Travis, C. S. Webster, and T. Nakamura, "Data Summary Report for Fission Product Release Test VI-4," NUREG/CR-5481 (ORNL/TM-11400), Oak Ridge National Laboratory, January 1991.
6. Osborne, M. F., R. A. Lorenz, J. R. Travis, C. S. Webster, and J. L. Collins, "Data Summary Report for Fission Product Release Test VI-5," ORNL/CR-5666 (ORNL/TM-11743), Oak Ridge National Laboratory, draft, December 1990.
7. Osborne, M. F., and R. A. Lorenz, "ORNL Studies of Fission Product Release Under LWR Accident Conditions," *Nuclear Safety*, 33(3):344-65, July-Sept. 1992.
8. Osborne, M. F., and R. A. Lorenz, "Fission Product Release at Severe Accident Conditions: FY 1989 Program Plan," ORNL/NRC/LTR-89/2, April 1989.
9. Lorenz, R. A., J. L. Collins, and S. R. Manning, "Fission Product Release from Simulated LWR Fuel," NUREG/CR-0274 (ORNL/TM-154), Oak Ridge National Laboratory, October 1978.
10. Osborne, M. F., J. L. Collins, F. A. Haas, R. A. Lorenz, J. R. Travis, and C. S. Webster, "Design and Final Safety Analysis Report for Vertical Furnace Fission Product Release Apparatus in Hot Cell B, Building 4501," NUREG/CR-4332 (ORNL/TM-9720), Oak Ridge National Laboratory, March 1986.
11. Croff, A. G., "ORIGEN2 — A Revised and Updated Version of the Oak Ridge Isotope Generation and Depletion Code," ORNL-5621, Oak Ridge National Laboratory, July 1980.
12. Lorenz, R. A., et al., "Prompt Release of Fission Products from Zircaloy-Clad UO<sub>2</sub> Fuels," Sect. 1 in *Nuclear Safety Program Annual Progress Report for the Period Ending December 31, 1987*, ORNL-4228, Oak Ridge National Laboratory, April 1988.
13. Collins, J. L., M. F. Osborne, R. A. Lorenz, and A. P. Malinauskas, "Fission Product Iodine and Cesium Release Behavior Under Severe LWR Accident Conditions," *Nucl. Technol.* 81(10):78-94 (1987).
14. Kuhlman, M. R., D. J. Lehmicke, and R. O. Meyer, "CORSOR User's Manual," NUREG/CR-4173 (BMI-2122), Battelle Memorial Institute, March 1985.
15. U.S. Nuclear Regulatory Commission, "Technical Bases for Estimating Fission Product Behavior During LWR Accidents," NUREG-0772, June 1981.
16. Osborne, M. F., R. A. Lorenz, and J. L. Collins, "Atmospheric Effects on Fission Product Behavior at Severe Accident Conditions," *Proc. Am. Nucl. Soc. Int'l. Top. Mtg. on the Safety of Thermal Reactors*, Portland, OR, July 21-25, 1991.
17. Osborne, M. F., and R. A. Lorenz, "Results of ORNL VI Series Fission Product Release Tests," *Proceedings of Twentieth Water Reactor Safety Information Meeting*, Bethesda, MD, October 21-23, 1992.

INTERNAL DISTRIBUTION

1. F. Barrera
2. E. C. Beahm
3. J. T. Bell
4. A. Boatman
5. C. W. Chase
6. J. L. Collins
7. T. A. Dillow
8. B. Z. Egan
9. W. Fulkerson
10. W. A. Gabbard
11. R. K. Genung
12. S. R. Greene
13. E. K. Johnson
14. T. S. Kress
- 15-19. R. A. Lorenz
20. A. P. Malinauskas
- 21-25. M. F. Osborne
26. G. W. Parker
27. C. E. Pugh
28. D. R. Reichle
29. J. C. Rudolph
30. R. P. Taleyarkhan
31. J. R. Travis
32. C. S. Webster
33. A. L. Wright
34. Central Research Library
35. ORNL—Y-12 Technical Library  
Document Reference Section
- 36-37. Laboratory Records
38. Laboratory Records, ORNL RC
39. ORNL Patent Section

EXTERNAL DISTRIBUTION

40. Office of Assistant Manager for Energy Research and Development, ORO-DOE, P.O. Box 2001, Oak Ridge, TN 37831
41. Director, Division of Reactor Safety Research, U.S. Nuclear Regulatory Commission, Washington, DC 20555
- 42-43. Office of Scientific and Technical Information, P.O. Box 2001, Oak Ridge, TN 37831
- 44-45. A. Behbahani, Accident Evaluation Branch, U.S. Nuclear Regulatory Commission, 5650 Nicholson Lane, Rockville, MD 20852
46. R. Y. Lee, U.S. Nuclear Regulatory Commission, Office of Nuclear Regulatory Research, NL344, Washington, DC 20555
47. R. Barrett, U.S. Nuclear Regulatory Commission, Office of Nuclear Reactor Regulation, OWFN, MS-8H7, Washington, DC 20555
48. J. H. Flack, U.S. Nuclear Regulatory Commission, Office of Nuclear Reactor Regulation, NLS324, Washington, DC 20555
49. L. Soffer, U.S. Nuclear Regulatory Commission, Office of Nuclear Reactor Regulation, NLS224, Washington, DC 20555
50. A. C. Thadani, U.S. Nuclear Regulatory Commission, Office of Nuclear Reactor Regulation, OWFN 8E2, Washington, DC 20555
51. E. S. Beckjord, U.S. Nuclear Regulatory Commission, Office of Nuclear Regulatory Research, NLS007, Washington, DC 20555
52. F. Eltawila, Accident Evaluation Branch, Office of Nuclear Regulatory Research, NLN344, Washington, DC 20555
53. N. Grossman, U.S. Nuclear Regulatory Commission, Office of Nuclear Regulatory Research, NLN344, Washington, DC 20555
54. T. L. King, U.S. Nuclear Regulatory Commission, Office of Nuclear Regulatory Research, NLN370, Washington, DC 20555

55. R. L. Palla, Jr., U.S. Nuclear Regulatory Commission, Office of Nuclear Regulatory Research, OWFN 10 E 4, Washington, DC 20555
56. B. W. Sharon, U.S. Nuclear Regulatory Commission, Office of Nuclear Regulatory Research, NLN369, Washington, DC 20555
57. T. P. Speis, U.S. Nuclear Regulatory Commission, Office of Nuclear Regulatory Research, NLS007, Washington, DC 20555
58. G. C. Tinkler, U.S. Nuclear Regulatory Commission, Office of Nuclear Regulatory Research, NLN344, Washington, DC 20555
59. M. D. Houston, U.S. Nuclear Regulatory Commission, Office of ACRS, PHIL P-315, Washington, DC 20555
60. A. M. Rubin, U.S. Accident Evaluation Branch, Office of Nuclear Regulatory Research, NLN344, Washington, DC 20555
61. B. Spencer, Argonne National Laboratory, 9700 South Cass Avenue, Argonne, IL 60439
62. W. H. Rettig, U.S. Department of Energy, Idaho Operations Office, 785 DOE Place, Idaho Falls, ID 83401-1134
63. C. Alexander, Battelle Columbus Laboratory, 505 King Avenue, Columbus, OH 43201
64. T. Pratt, Brookhaven National Laboratory, 130 BNL, Upton, NY 11973
65. M. Merilo, Electric Power Research Institute, P.O. Box 10412, 3412 Hillview Avenue, Palo Alto, CA 94304
66. R. J. Hammersley, Fauske and Associates, Inc., 16WD70 West 83rd Street, Burr Ridge, IL 60521
67. F. E. Panisko, Reactor Systems, Fuels & Materials, P8-35, Pacific Northwest Laboratory, P.O. Box 999, Richland, WA 99352
68. N. Bixler, Sandia National Laboratory, P.O. Box 5800, Albuquerque, NM 87185
69. D. Powers, Sandia National Laboratory, P.O. Box 5800, Albuquerque, NM 87185
70. S. Thompson, Sandia National Laboratory, P.O. Box 5800, Albuquerque, NM 87185
71. K. Washington, Sandia National Laboratory, P.O. Box 5800, Albuquerque, NM 87185
72. K. O. Reil, Sandia National Laboratory, P.O. Box 5800, Albuquerque, NM 87185
73. I. Catton, University of California Los Angeles, Nuclear Energy Laboratory, 405 Hilgard Avenue, Los Angeles, CA 90024
74. C. M. Allison, Idaho National Engineering Laboratory, EG&G Idaho, Inc., P.O. Box 1625, MS 3840, Idaho Falls, ID 83415
75. R. Schneider, ABB/CE, 1000 Prospect Mill Road, CEP 9612-2207, Winsor, CT 06095
76. D. Buttermer, PLG Inc., 191 Calle Magdalena, Suite 240, Encinitas, CA 92024
77. James Metcalf, Stone and Webster, 245 Summer Street, MS 245-2, Boston, MA 02107
78. John Conine, G. E. Knolls Atomic Power Laboratory, Box 1072, D2-221, Schenectady, NY 12501
79. J. Sugimoto, Japan Atomic Energy Research Institute, Tokai-mura, Naka-gun, Ibaraki-ken, 319-11, Japan
80. Hee-Dong Kim, Nuclear Safety Division, Korea Advanced Energy Research Institute, P.O. Box 7, Daeduk Danji, Taejeon 305-353, Korea
81. Kenji Takumi, Nuclear Power Engineering Center, Fujitakanko Building, 17-1 3-Chrome, Toranomon, Minato-Ku, Tokyo 105, Japan
82. J. W. Wolfe, Westinghouse Bettis Atomic Laboratory, P.O. Box 79, ZAP 34N, West Mifflin, PA 15122
83. S. Inamati, General Atomics, P.O. Box 85608, San Diego, CA 92138-5608
84. M. Kazimi, Massachusetts Institute of Technology, Nuclear Engineering Department, 77 Massachusetts Avenue, Cambridge, MA 02139
85. N. Todreas, Massachusetts Institute of Technology, Nuclear Engineering Department, 77 Massachusetts Avenue, Cambridge, MA 02139
86. E. Stubbe, Belgonucleaire, Department of LWR Fuel, Rue de Champde Mars 25, B-1050 Brussels, Belgium
87. L. A. Simpson, Whiteshell Laboratories AECL Research, Reactor Safety Research Division, Pinawa, Manitoba, Canada ROE 1L0
88. Peter Hofmann, Institute of Materials & Solid State Research, Kernforschungszentrum Karlsruhe, P.O. Box 3640, D-7500 Karlsruhe 1, Germany
89. Bernhard Kuczera, Nuclear Safety Research Project (PSF), Kernforschungszentrum Karlsruhe, P.O. Box 3640, D-7500 Karlsruhe 1, Germany

90. G. Petrangeli, Nucleare e della Protezione Sanitaria, Ente Nazionale Energie Alternative, Viale Regina Margherita, 125, Casella Postale M. 2358, I-00100 Roma A.D., Italy
91. S. I. Chang, Institute of Nuclear Energy Research, P.O. Box 3, Lungtan, Taiwan 325, Republic of China
92. J. Bagues, Consejo de Seguridad Nuclear, JOR Angela de la Cruz No 3, Madrid 28056, Spain
93. A. Alonso, E.T.S. Ingenieros Industriales, Jost Gutierrez Abascal, 2, 28006 Madrid, Spain
94. W. Frid, Statens Karnkraftinspektion, P.O. Box 27106, S-10252 Stockholm, Sweden
95. K. J. Brinkman, Reactor Centrum Nederland, 1755 ZG Petten, The Netherlands
96. Paola Fasoli-Stella, Thermodynamics and Radiation Physics, CEC Joint Research Center, Ispra, I-201020 Ispra (Varese), Italy
97. P. Vaisnys, VATESI, Gediminis Prospect 36, Vilnius, Lithuania
98. S. Elo, Hungarian Atomic Energy Commission, H-1374 Budapest, P.O. Box 565, Budapest, Hungary
99. J. Stuller, State Office for Nuclear Safety, Slezska 9, 1200 00 Prague 2, Czech Republic
100. S. Kinnersly, UKAEA, Winfrith, Dorchester DT2-8DH, Dorset, England
101. D. Williams, UKAEA, Winfrith, Dorchester DT2-8DH, Dorset, England
102. J. A. Martinez, Consijo de Seguridad Nuclear, Justo Dorado 11, 28040 Madrid, Spain
103. V. Asmolov, I.V. Kurchatov Institute of Atomic Energy, Nuclear Safety Department, Moscow 123182, Russia
104. M. LiVolant, Institut de Protection et de Surete Nucleaire, CEN/FAR - B.P. No 6, F-92265, Fontenay-aux-Roses, Cedex, France
105. P. Hosemann, Paul Scherrer Institute, Programm LWR-Sicherheit, CH-5232 Villigen, PSI, Switzerland
106. Y. Yanev, Committee on the Use of Atomic Energy for Peaceful Purposes, 69 Shipchenski, Prokhd Blvd., 1574, Sofia, Bulgaria
107. J. Misak, Nuclear Regulatory Authority, Slovak Republic, Bajkalska 27, 827 21 Bratislave, Solvak Republic
108. A. Meyer-Heine, Cadarache Center for Nuclear Studies, F-13108 Saint Paul-Lez-Durance Cedex, France
109. J. Leveque, DTP/SECC/LESC, Centre d'Etudes Nucleaires de Grenoble, 85X - 38041 Grenoble Cedex, France
110. B. Andre, Service d'Etude du Comportement des Combustibles, Centre d'Etudes Nucleaire de Grenoble, 17 Rue de Martyrs, 38054 Grenoble Cedex 9, France
111. S. Chakraborty, Swiss Federal Nuclear Safety Inspectorate, CH-5232 Villigen - HSK, Switzerland
112. P. Kloeg, N.V. Kema, P.O. Box 9035, 6800 ET ARNHEM, The Netherlands
113. L. Bolshov, Russian Academy of Sciences, Nuclear Safety Institute, 52, 8, Tulskaaya, Moscow, 113191, Russia
114. E. Cordfunke, Netherlands Energy Research Foundation, P.O. Box 1, 1755 ZG Petten, The Netherlands
115. B. Mavko, Jozef Stefan Institute, Jamova 39, 61111 Ljubljana, Slovenia, Czechoslovakia
116. P. Stoop, Netherlands Energy Research Foundation, P.O. Box 1, 1755 ZG Patten, The Netherlands
117. K. S. Norwood, 8 Appleford Drive, Abingdon, Oxon OX14, 2DA, United Kingdom
118. S. J. Wisbey, B.220, AERE Harwell, Didcot, Oxon OX11 ORA, United Kingdom
119. T. Yamashita, Nuclear Fuel Chemistry Laboratory, Department of Chemistry, Japan Atomic Energy Research Institute, Tokai-mura, Naka-gun, Ibaraki-ken, 319-11, Japan
120. S. Hagen, Bau 601, Kernforschungszentrum Karlsruhe, Postface 3640, D7500 Karlsruhe 1, Federal Republic of Germany
121. M. L. Brown, 15 Barrock St., Thurso Caithness, Scotland KW14 7DB
122. T. Nakamura, Japan Atomic Energy Research Institute, Reactivity Accident Laboratory, Department of Fuel Safety Research, Tokai Research Establishment, Tokai-Mura, Naka-Gun, Ibaraki-Ken, Japan 319-11
123. H. K. Lee, Spent Fuel Storage and Disposal Technology Section, Korea Advanced Energy Research Institute, P.O. Office Box 7, Dae-Danji Choong-Nam, Republic of Korea
124. Y.-C. Tong, Institute of Nuclear Energy Research, P.O. Box 3-6, Lung-Tan, Taiwan, Republic of China
125. A. Nichols, Technology Division, AEE Winfrith, Dorchester, Dorset, England
126. D. Williams, Technology Division, AEE Winfrith, Dorchester, Dorset, England
127. F. C. Inglesias, AECL, Chalk River Nuclear Laboratories, Chalk River, Ontario, KOJ 1JO, Canada
128. R. R. Hobbins, EG&G Idaho, Inc., P.O. Box 1625, Idaho Falls, ID 83401
129. D. A. Petti, EG&G Idaho, Inc., P.O. Box 1625, Idaho Falls, ID 83401
130. D. J. Osetek, Los Alamos Technical Associates, Inc., 2400 Louisiana Blvd. N.E., Building 1, Suite 400, Albuquerque, NM 87110.
131. L. A. Neimark, Argonne National Laboratory, 9700 South Cass Ave., Argonne, IL 60439

132. J. Rest, Argonne National Laboratory, 9700 South Cass Ave., Argonne, IL 60439
133. Y. Y. Liu, Argonne National Laboratory, 9700 South Cass Ave., Argonne, IL 60439
134. K. Y. Suh, Fauske & Associates, Inc., 16W070 West 83rd St., Burr Ridge, IL 60521
135. D. S. Cox, Chalk River Laboratories, Chalk River, Ontario, Canada K0J 1J0
136. B. J. Lewis, Department of Chemistry and Chemical Engineering, Royal Military College of Canada, Kingston, Ontario K7K 5L0, Canada
137. B. R. Bowsher, AEA Technology, Winfrith, Dorchester, Dorset DT2 8DH, United Kingdom
- 138-387. Given distribution as shown in Category R3 (NTIS - 10)

NRC FORM 335  
(2-89)  
NRCM 1102  
3201, 3202

U.S. NUCLEAR REGULATORY COMMISSION

# BIBLIOGRAPHIC DATA SHEET

(See instructions on the reverse)

1. REPORT NUMBER  
(Assigned by NRC, Add Vol., Supp., Rev.,  
and Addendum Numbers, if any.)

NUREG/CR-6077  
ORNL/TM-12416

2. TITLE AND SUBTITLE

Data Summary Report for Fission Product Release Test VI-6

3. DATE REPORT PUBLISHED

MONTH	YEAR
March	1994

4. FIN OR GRANT NUMBER

B0127

5. AUTHOR(S)

M. F. Osborne, R. A. Lorenz, J. R. Travis, C. S. Webster,  
and J. L. Collins

6. TYPE OF REPORT

Technical

7. PERIOD COVERED (Inclusive Dates)

8. PERFORMING ORGANIZATION - NAME AND ADDRESS (If NRC, provide Division, Office or Region, U.S. Nuclear Regulatory Commission, and mailing address; if contractor, provide name and mailing address.)

Oak Ridge National Laboratory  
Oak Ridge, TN 37831-6050

9. SPONSORING ORGANIZATION - NAME AND ADDRESS (If NRC, type "Same as above"; if contractor, provide NRC Division, Office or Region, U.S. Nuclear Regulatory Commission, and mailing address.)

Division of Systems Research  
Office of Nuclear Regulatory Research  
U.S. Nuclear Regulatory Commission  
Washington, DC 20555-0001

10. SUPPLEMENTARY NOTES

11. ABSTRACT (200 words or less)

Test VI-6 was the sixth test in the VI series conducted in the vertical furnace. The fuel specimen was a 15.2-cm-long section of a fuel rod from the BR3 reactor in Belgium. The fuel had experienced a burnup of ~42 MWd/kg, with inert gas release during irradiation of ~2%. The fuel specimen was heated in an induction furnace at 2300 K for 60 min, initially in hydrogen, then in a steam atmosphere. The released fission products were collected in three sequentially operated collection trains designed to facilitate sampling and analysis.

The fission product inventories in the fuel were measured directly by gamma-ray spectrometry, where possible, and were calculated by ORIGEN2. Integral releases were 75% for <sup>85</sup>Kr, 67% for <sup>129</sup>I, 64% for <sup>125</sup>Sb, 80% for both <sup>134</sup>Cs and <sup>137</sup>Cs, 14% for <sup>154</sup>Eu, 63% for Te, 32% for Ba, 13% for Mo, and 5.8% for Sr. Of the totals released from the fuel, 43% of the Cs, 32% of the Sb, and 98% of the Eu were deposited in the outlet end of the furnace. During the heatup in hydrogen, the Zircaloy cladding melted, ran down, and reacted with some of the UO<sub>2</sub> and fission products, especially Te and Sb. The total mass released from the furnace to the collection system, including fission products, fuel, and structural materials, was 0.57 g, almost equally divided between thermal gradient tubes and filters. The release behaviors for the most volatile elements, Kr and Cs, were in good agreement with the ORNL Diffusion Model.

12. KEY WORDS/DESCRIPTORS (List words or phrases that will assist researchers in locating the report.)

Fission product  
Fission product release  
Fuel damage

13. AVAILABILITY STATEMENT

Unlimited

14. SECURITY CLASSIFICATION

(This Page)

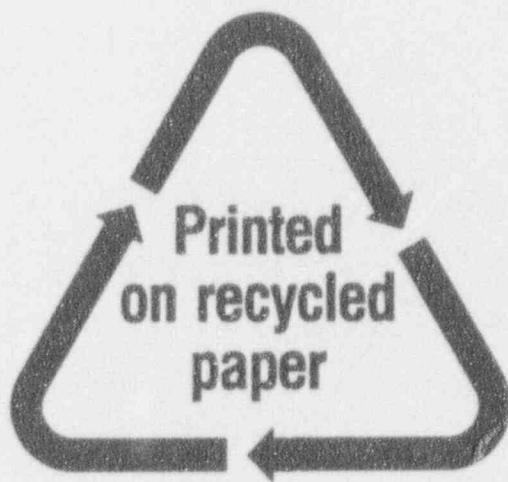
Unclassified

(This Report)

Unclassified

15. NUMBER OF PAGES

16. PRICE



Federal Recycling Program

UNITED STATES  
NUCLEAR REGULATORY COMMISSION  
WASHINGTON, D.C. 20555-0001

OFFICIAL BUSINESS  
PENALTY FOR PRIVATE USE, \$300

FIRST CLASS MAIL  
POSTAGE AND FEES PAID  
USNRC  
PERMIT NO. G 67

120555139531 1 JAN 94  
US NRC-OADM  
DIV FOIA & PUBLICATIONS SVCS  
TPS-PDR-NUREG  
P-211  
WASHINGTON DC 20555